Univerzita Karlova v Praze
Přírodovědecká fakulta

Studijní program: Biologie
Studijní obor: BBI (1501R001)

Filip Tomáška

Moderní optické *in vivo* metodiky v neurofyziologickém výzkumu

Modern optical *in vivo* methods in neurophysiological research

Bakalářská práce

Vedoucí bakalářské práce: Mgr. Ondřej Novák

Praha, 2016

Prohlášení:

Prohlašuji, že jsem závěrečnou práci zpracoval samostatně a že jsem uvedl všechny použité informační zdroje a literaturu. Tato práce ani její podstatná část nebyla předložena k získání jiného nebo stejného akademického titulu.

V Praze, 12.05.2016

Podpis

Poďakovanie:

Rád by som poďakoval Mgr. Ondřejovi Novákovi za jeho trpezlivú pomoc od zadania práce až po jej finálne úpravy. Vďaka patrí taktiež mojej rodine za ich podporu a cenné rady.

Abstract

Accurate visualization of structures and events at subcellular level is one of the major challenges of current neuroscience. Optical methods based on fluorescence imaging were optimized to record and control neural activity, thus presenting a powerful approach complementary to historically dominant electrophysiological techniques. The employment of two-photon excitation enabled *in vivo* imaging of neurons up to 1 mm from the sample surface without causing significant photodamage. The application of methods of molecular biology has yielded protein-based genetically targetable indicators of neural activity, possessing performance comparable to the traditional organic dyes. Moreover, heterologous expression of microbial opsins proved capable of light-induced neural excitation or silencing in a single-component manner. The combination of these optogenetic tools offers two-way control over neuronal populations with single cell resolution. If coupled with calcium or voltage fluorescent indicators and transgenic animal models, such systems represent a non-invasive, all-optical tool for simultaneous control and imaging of specific neuronal subtypes. Its application supported by electrical recordings may finally provide the data necessary for the uncovering of fundamental principles of neural functioning.

Key words: neurophysiological models, transgenic animals, two-photon microscopy, optophysiology, synthetic indicators, genetically encoded indicators, optogenetics

Abstrakt

Jednou z hlavných výziev dnešných neurovied je presná vizualizácia štruktúr a procesov na sub-bunkovej úrovni Optické metódy založené na fluorescenčnom zobrazovaní optimalizované na záznam a ovládanie neuronálnej aktivity predstavujú prístup doplňujúci tradičné elektrofyziologické techniky. Použitie dvojfotónovej excitácie umožnilo zobrazovanie neurónov *in vivo* až do hĺbky 1 mm od povrchu vzorky a to bez významného poškodenia svetlom. Aplikácia metód molekulárnej biológie viedla k vytvoreniu proteínových indikátorov neurálnej aktivity, ktoré dnes už disponujú vlastnosťami tradičných syntetických farbív. Heterológna expresia mikrobiálnych opsínov umožňuje svetlom ovládané vyvolanie nervových vzruchov, alebo ich útlm za pomoci jediného komponentu. Kombinácia týchto optogenetických nástrojov poskytuje dvojsmernú kontrolu nad neurálnou aktivitou s rozlíšením na úrovni jednej bunky. V kombinácii s vápnikovým alebo napäťovým zobrazovaním neurálnej aktivity a transgénnymi zveracími modelmi takýto systém predstavuje neinvazívny optický nástroj schopný súčasného záznamu a kontroly neuronálnej aktivity. Jeho použitie podporené elektrickým záznamom, by mohlo viesť k pochopeniu základných princípov funkcie nervovej sústavy.

Kľúčové slová: neurofyziologické modely, transgénne zvieratá, dvojfotónová mikroskopia, optofyziológia, syntetické indikátory, geneticky kódované indikátory, optogenetika

Table of contents

1 Introduction

The origins of modern neuroscience are closely linked to a method capable of visualizing populations of cells in their native morphology. It was the staining method developed by Camillo Golgi that presented Santiago Ramón y Cajal with the key to discoveries ultimately resulting in the neuron doctrine. The following century was dominated by electrophysiology, extensively describing the electrical properties of single excitable cells.

Today, 100 years after the neuron doctrine, novel optical methods capable of visualizing and control over neural activity of hundreds of cells have emerged. In combination with transgenic animal models, these methods are now capable of large-scale neural activity imaging and control *in vivo*, possibly presenting us with a similarly powerful tool capable of similarly redefining impact.

The main motivation of this text is to review the tools and techniques capable of visualization and control over neural activity. These include transgenic model organisms, various methods of fluorescence microscopy (most notably the two-photon laser-scanning microscope), synthetic and protein-based optophysiological probes and optogenetics.

2 Animal models

In vivo experiments on animal models are an indispensable tool for understanding the function of neural tissue. The following table provides a list of model organisms along with their general characteristics.

Table.1, A list of the most commonly used animal models in neuroscience along with their general characteristics (Riddle et al., 1997; Lambert, 2007; Wheeler and Brandli, 2009; IOM and NRC, 2012; Stewart et al., 2014)

	Generation time	**Litter size**	**Relation to human**	**Cost of care**	**General pros**	**General cons**
C.elegans	4 days	300/4 days	Nematode, weakest relation	Minimal; freezable stocks	Constant number and fate of cells, transparent,	Absence of site directed mutagenesis, simple nervous system
Drosophila	10 days	500 eggs/30 days lifespan	Insect, poor relation	minimal	Good genetic tools available, cheap	Discoveries may require revisiting if they are to be applied to humans
Zebrafish	2-4 months	100-200 eggs/week	Vertebrate, worse than mice	0,67$/month/fish	Transparent, easy to keep	Poor reverse genetics
Mouse (Rat)	6-8 weeks	5-10 (6-12) pups/litter 5-10 times/year	Close - mammals, worse than macaque	High compared to other models (aprox.1 $/day)	Transgenic animals, nervous system close to humans	Anatomical difference in selected CNS structures. Poor access to embryo
Rhesus macaque	12 years	1 /year	An old world monkey, therefore the closest	Very high. 30 000 $ for acquisition and 80 - 110$/day for keeping	The closest nervous system organization and function.	Very expensive to purchase and keep. Ethical restrictions

Caenorhabditis elegans is a nematode of microscopic size, possessing a simple nervous system. It has very low requirements for care since it can be cultivated in large numbers on agar and kept in frozen stocks. The constant fate and number of its cells made it into a widely studied developmental model. Furthermore, its relevance in neuroscience is increased by the fact that it is the only model organism of which the whole connectome has been mapped by serial section electron microscopy (White et al., 1986). Thus, making it a simple model for studying fundamental principles of neural tissue function, such as basic sensorimotor circuits responsible for modulating motor activity based on sensory input (Sengupta and Samuel, 2009).

Drosophila melanogaster (fruit fly), is an insect which does not require extensive care and its keeping does not represent a significant economic burden. Forward genetics experiments conducted on *D. melanogaster* have led to the discovery of many genes active in neural development such as the Notch signaling pathway (Poulson, 1950), active in cell fate regulation (Breunig et al., 2007). Similar to *C.elegans*, it cannot provide detailed information about the function of the vertebrate brain; however, it may help understand fundamental principles of neural function and organization (Bellen et al., 2010). For example, neural circuits active in the sexual behavior (courtship behavior) of fruit flies are studied to better understand how sensory input is processed and how the associated motor output is generated (Pavlou and Goodwin, 2013).

Danio rerio, a teleost fish, can be characterized as a relatively new and, in terms of care, the least demanding vertebrate model (Streisinger et al., 1981). Similarly to *C.elegans* and *Drosophila*, maintenance of large numbers of zebrafish (*D.rerio)* is possible, which enables large-scale genetic experiments in developmental research (Driever et al., 1996). Nevertheless, zebrafish has also been a model for neural development on a cellular level (Kimmel, 1993), in vertebrate neural wiring principles (Kita et al., 2015), and in basic behavioral studies (Guo, 2004). These include the discovery of right eye preference in biting (Miklosi and Andrew, 1999) or a memory assessment proving zebrafish is a relevant model in learning experiments (Williams et al., 2002).

Until the mid-1980s, feline models represented the largest fraction of animals used in neuroscience mainly due to their ability to withstand complicated surgical procedures using large instruments. However, negative public opinion about experimentation on companion animals and strict regulations have increased the cost of their use.

Miniaturized equipment and the appearance of transgenic mice (Capecchi, 1989) have transformed rodents, such as *Mus musculus* (mouse) and *Rattus norvegicus* (rat), into the default animal model of neuroscience. Rodents are mammals; therefore, their relevance in terms of neural organization surpasses all listed models (Tab.1) except the non-human primates (NHPs). Moreover, the difference between rodent and NHP brain anatomy was shown not to be completely restrictive in terms of studying cognition (Kepecs et al., 2008). Consequently, the majority of research in neuroscience, including areas such as cell-fate determination or neural circuit wiring (Kabanova et al., 2015), can profit from the rodent model.

The non-human primates (NHPs) such as *Macaca mulatta* (rhesus macaque) are the most expensive and challenging animal model to keep. The main topographical and functional brain structures responsible for sensory, motor or attention processing appeared early enough in the evolution and are conserved among primates (Mantini et al., 2013). Information from NHPs can be often directly applied to humans. However, because of the high cost and limiting regulations, only a minority of the research is performed on NHPs (Roelfsema and Treue, 2014), while being restricted to areas where rodent models cannot provide relevant data such as higher visual sensory processing and attention (Moore and Armstrong, 2003).

3 Related molecular biology

3.1 Gene targeting

Visualizations of different cell types *in vivo*, or pathology-related studies in neuroscience require the expression of exogenous genes by the cells of the model organism. In general, modification of genomic DNA, such as the insertion of an exogenous gene, is achieved through the *in vitro* introduction of a gene-of-interest-containing vector into the cell (e.g. embryonic stem (ES) cell), by electroporation (Neumann et al., 1982) or microinjection (Gordon et al., 1980). However, random integration of the construct may cause disruption of a potentially crucial coding region, which may lead to an altered phenotype. Furthermore, the expression of the transgene is influenced by many factors other than the promoter, such as missing regulatory sequences or different chromatin architecture (Huang, 2010). It is, therefore, preferable to target the exogenous gene by surrounding it with a specific sequence representing the context in which it should appear on the chromosome. Consequently, the disruption is limited to a specifically targeted gene, while all its regulatory sequences are transferred to the insert (Huang, 2010).

The retention of the targeted gene may be required in cases where cell-type specific proteins are selected. Since the presence of these proteins often defines the otherwise thin lines between cell types, their further functionality is indispensable (Taniguchi et al., 2011). To avoid the loss of function of the targeted gene, the exogenous gene may be linked to its target by a bicistronic cassette (IRES (internal ribosome entry site), 2A); a short sequence of viral origin capable of manipulating the translational apparatus so that two proteins are co-expressed from a single mRNA, transcription of which is controlled by the endogenous gene promoter (Pelletier and Sonenberg, 1988; Radcliffe and Mitrophanous, 2004; Provost et al., 2007).

3.2 In vivo application

The integrated construct contains a selection cassette (such as the neomycin resistance) so that the cells where integration occurred can be selected on a selection medium and injected into the blastocoel of a host embryo, which is then placed into the uterus of a foster mother (Thomas and Capecchi, 1987; Capecchi, 1989). The resulting animal is a chimera containing modified ES cell descendants along with host embryo cells. If the germ-line cells are transgenic, further breeding leads to a homozygous animal.

Postnatal *in vivo* gene delivery is possible by exploiting the native ability of viral vectors to express their genes in host cells. Lentiviral (LV) expression vectors are capable of infecting non-dividing cells as opposed to the rest of the retroviruses (Wollebo, 2013). Since they integrate into the genome these vectors offer stable expression of transgenes up to 10 kbp long, within hours after transduction (Karra and Dahm, 2010). However, the integration lacks specificity and may result in insertional mutagenesis (Karra and Dahm, 2010). The naturally non-pathogenic adeno-associated virus (AAV)-based vector is capable of transducing the host cell with a gene of ~5kbp (Karra and Dahm, 2010). Nevertheless, cell-type specificity limited by the length of the construct, can be compensated by choosing among various available serotypes with different tropisms (Shevtsova et al., 2005). AAV-based vectors lack the sequences responsible for integration into the genome and therefore persist episomally (Buning et al., 2008), thus causing multiple-week long transient expression. The expression of transduced genes is high, while the immune reaction is minimal, although the onset of expression is up to 2 weeks (Karra and Dahm, 2010).

3.3 Control over transgene by site-specific recombinases (SSRs)

The transgene affects the cells in which it is expressed. The cell has to spend considerable amount of its limited energy and resources on an unnecessary and possibly toxic product. If expressed (or overexpressed) in every cell from the early embryogenesis the transgene may affect ontogenesis resulting in abnormal development (McHenry et al., 1998).

Tyrosine SSRs of the integrase family are capable of providing control over the transgene expression, thus minimizing its negative effect. Cre, a 34kDa SSR from the P1 bacteriophage, recognizes two loxP sites consisting of a spacer sequence and two palindromic sequences on the sides with the total length of 34 bp (Sternberg and Hamilton, 1981; Sauer and Henderson, 1988). Analogously, Flp, a SSR from the 2µm plasmid of *S.cerevisiae*, recognizes two frt sites consisting of two 13bp inverted repeats separated by an asymmetrical 8bp spacer. (Schwartz and Sadowski, 1989; Sadowski, 1995). Depending on the relative orientation of the two recognition sites (loxP or frt), the sequence between them can be either excised/inserted, inverted or translocated (Fig. 1).

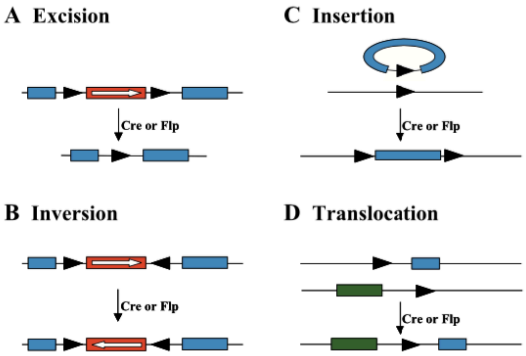

Fig. 1, An overview of reactions mediated by SSRs along with the corresponding relative orientations of their recognition sites (Bockamp et al., 2002).

3.3.1 Conditional transgenesis – spatial control

Conditional transgenesis is a method where the transgene is inactivated by default, thus eliminating its possible influence on ontogenesis. A loxP (or frt) flanked stop cassette is inserted between the promoter and the rest of the coding sequence. The excision of the stop cassette, only possible in Cre (or Flp) expressing cells, initiates the gene-of-interest transcription. The promoter controlling the expression of the SSR, therefore regulates the spatial aspect of the transgene expression (Lakso et al., 1992). A knock-in animal with such tissue-specific Cre activity (driver line) can be mated with a reporter-line animal containing a *loxP-STOP-loxP-gene of interest* knock-in. Their offspring will possess a heterozygous set of alleles where Cre will deactivate/activate the knock-in gene of interest, in a tissue specific manner (Orban et al., 1992).

3.3.2 Viral transduction by a SSR

Viral transduction may be combined with the Cre/loxP (or Flp/frt) system upon creating an alternative approach in conditional transgenesis (Ahmed et al., 2004). If a Cre-containing LV- or AAV-based vector transduces a reporter mouse, the stop cassette is excised only in the specific cell-type to which the viral vector was targeted (Ahmed et al., 2004). Alternatively, a viral vector containing the flanked STOP cassette can transduce a driver mouse with specific Cre expression (Kuhlman and Huang, 2008). The expression of the gene-of-interest is therefore limited to the injection site and time along with the genetically targeted cell-type.

3.3.3 Temporal control

To achieve temporal control over the expression of the gene-of-interest, ligand-activated SSRs have been developed. A chimeric Cre recombinase has been constructed by fusing the recombinase with a mutated human estrogen receptor ligand-binding domain. This construct is activated by a synthetic ligand, tamoxifen (Feil et al., 1997), which can be injected at a certain time achieving temporal specificity of the conditional transgene (Hayashi and McMahon, 2002).

3.4 Tetracycline-based expression control

Apart from the SSR-based expression control, the tetracycline dependent tetOFF/tetON regulation is available. By fusing an *E.coli* tetracycline responsive tet repressor to a *Herpes simplex* virion protein (its activating domain), a tetracycline-dependent transactivator (tTA) was created. The tTA transactivator binds to a tetO operator sequence upstream from a promoter, which initiates the gene expression. In the case of tetOFF, tetracycline (or its derivative doxycycline) prevents the tTA from binding tetO (Gossen and Bujard, 1992) (Fig. 2a). However, in the case of tetON, a mutant tTA binds the tetO operator only in the presence of tetracycline (or one of its derivatives) (Fig. 2b) (Gossen et al., 1995).

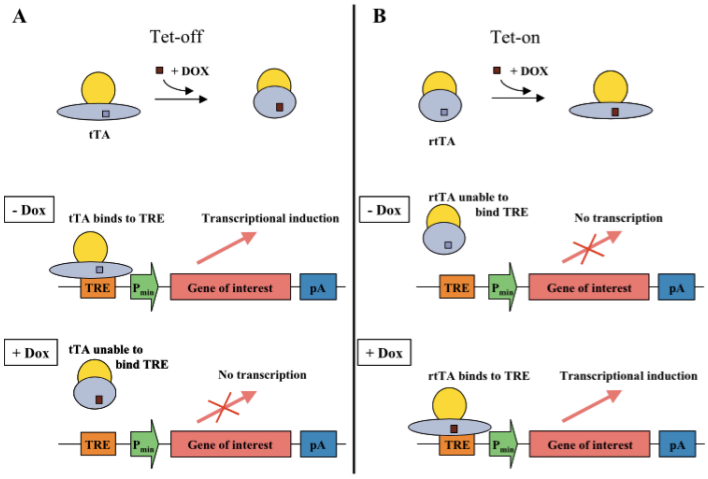

Fig.2. Schematic representation of Tet-off (*a*) Tet-on (*b*) systems. (tTA) tetracycline-dependent transactivator; (rtTA) modified tTA; (TRE) tetO operator (Bockamp et al., 2002).

4 Fluorescence Microscopy (FM)

Fluorescence microscopy (FM) relies on the presence of a fluorescent agent in the imaged tissue. In the case of one-photon FM, these agents are able to absorb light of a specific excitation wavelength and subsequently emit a photon of a longer wavelength (Stokes shift). The emitted light is detected by the microscope and defines spatiotemporal properties of the studied structure. The specific manner of interaction between the fluorescent molecule and the element of interest, results in augmented contrast between the studied structure and the background. This contrast helps visualizing structures otherwise barely visible in bright-field (for example the visualization of nuclei by DAPI (4',6-diamidino-2-phenylindole)).

4.1 Wide-field Fluorescence Microscopy (WFFM)

WFFM is a relatively simple and inexpensive FM method. A basic WFFM setup includes a powerful light source (monochromatic lamp), an excitation and emission filter and a dichroic mirror. The last three components are usually combined within a replaceable cube. Advantages of a WFFM setup in comparison with other FM approaches include lower price and usually fast temporal resolution (provided using cooled CCD (charge coupled device) or EMCCD (electron multiplying CCD) cameras) (Combs, 2010). On the other hand, WFFM is not capable of optical sectioning since the untraceable signal from deeper layers of the sample contaminates the relevant fluorescence from the focal plane (Fig. 4) (Combs, 2010), therefore significantly lowering the resolution.

4.2 Laser Scanning Confocal Microscopy (LSCM)

LSCM is capable of optical sectioning by eliminating the problematic out-of-focus fluorescence before it reaches the detector through two small apertures, “pinholes”. Both pinholes are in planes conjugate to the focal plane (Combs, 2010), while the illuminating pinhole narrows down the laser beam.

The emission pinhole is in the exact position so that only light originating from the focal plane may pass through the opening into the photomultiplier tubes (PMTs) (Shaw, 1995) (Fig. 3)

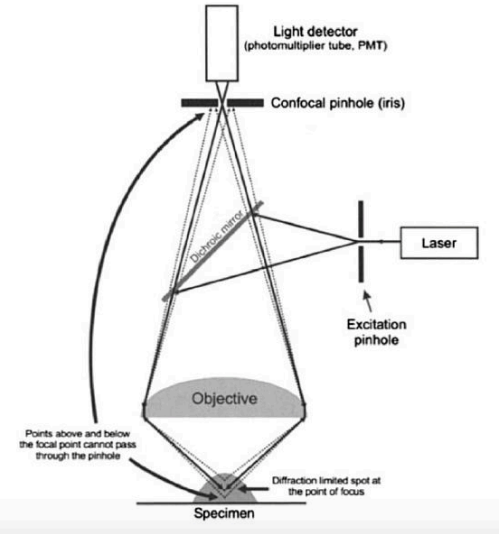

Fig. 3, A schematic diagram of a LSCM setup (Shaw, 1995).

The main advantage of LSCM lies within its axial and lateral resolution (near diffraction-limit) capable of high-resolution optical scanning in thin samples (Fig. 4). Also, LSCM supports a wide range of sample types, for example enabling precise sub-cellular 3D imaging of the intracellular pH regulation in continuously superfused cancer cells (Hulikova et al., 2011). On the other hand LSCM has slower scanning speed and its imaging depth is significantly limited by intense excitation light scattering resulting in signal loss (Combs, 2010). Thus, LSCM is not optimal for imaging of fast events such as fast trains of action potentials, or for deep-tissue imaging.

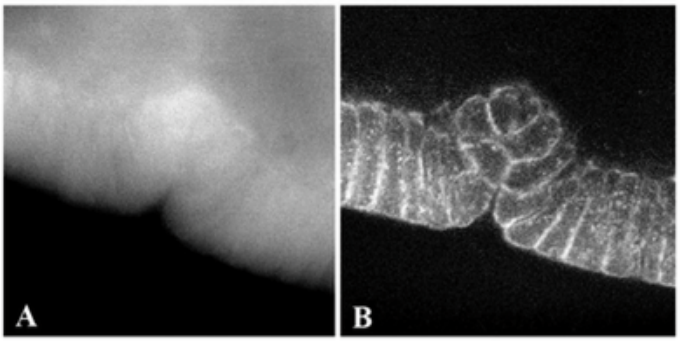

Fig. 4, Two images of the same *Drosophila* embryo with rhodamine-phalloidin labeled actin. A wide-field fluorescence microscope with cooled CCD camera was used to obtain image A while a confocal microscope was used to obtain image B (Shaw, 1995) Light scattering makes it impossible to determine which photons originate from the focal plane and results in blurry images (A). In the case of LSCM, the increasing amount of scatter results in decreasing signal since more light has to be filtered out by pinhole.

4.3 Non-linear optical microscopy

Non-linear excitation optical microscopy generates signal via light-fluorophore interactions involving multiple photons (multiphoton absorption) simultaneously (~fs) interacting with the fluorophore

upon its excitation. The most probable and widely used non-linear process used in FM is the two-photon absorption (2PA).

4.3.1 Quantum mechanics behind two-photon absorption (2PA)

The absorption or emission of a photon is usually mediated by transitions in electronic states of π-conjugated electrons of the chromophore. The absorption of a photon (or a combined energy of two-photons (2PA)) leads to a transition in the electronic state of π-conjugated electrons from a ground state (S_0) to an excited state (S_n). Subsequent relaxation firstly leads to reaching the first excited state (S_1). This relaxation is very fast (~10^{-12}s) and non-radiative. Fluorescence is emitted only by the slower (~10^{-9}s) relaxation from S_1 to the ground state (S_0), usually not ground vibrational state, regardless of which excited high-energy state (S_n) was reached by absorption (Vavilov-Kasha's rule) (Drobizhev et al., 2011) (Fig. 5).

The Jablonski diagram (Fig. 5) demonstrates how two photons of a longer wavelength combine their energies in 2PA, causing the electronic transition of the chromophore similar to the one caused by one-photon absorption. Both 1PA and 2PA finally generate the same fluorescence during relaxation even though the combination of wavelengths in 2PA may not be equal to the 1PA wavelength.

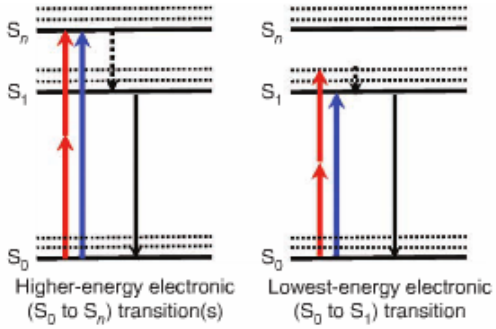

Fig. 5, A Jablonski diagram representing two- and one-photon absorption during low- and high-energy electronic transitions (Drobizhev et al., 2011),. Generated fluorescence remains constant due to Vavilov-Kasha's rule.

4.3.2 The probability of 2PA and its consequences

In two-photon excitation (2PE), the absorption probability and, subsequently, the amount of emitted fluorescence is proportional to the square intensity of incident light (Zipfel et al., 2003). Therefore, it decreases with the second power of axial distance (z) ($1/z^2$) from the focal plane (Eq. 1) (Fig. 6) (Tsai and Kleinfeld, 2009).

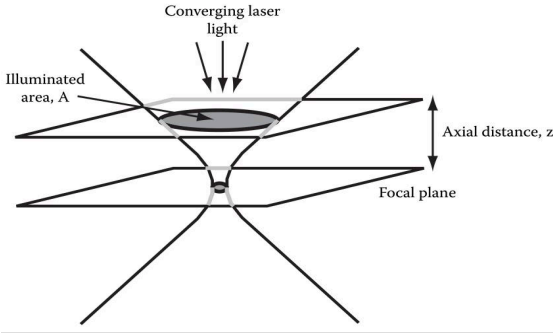

$$F_{total} \propto I^2 A \propto \left(\frac{P}{z}\right)^2$$

Fig. 6, Eq. 1, Elements contributing to the localization of 2PE in Eq. 1. The missing factor "*P"* represents laser power (Tsai and Kleinfeld, 2009)

In summary, the probability of 2PA decreases rapidly with distance from the focal plane, while the area where fluorescence is generated is restricted to a near-diffraction limited focal spot (Denk et al., 1990), thus eliminating the need for a pinhole (Mainen et al., 1999). Optical sectioning is achieved solely by the spatially limited occurrence of fluorophore excitation (Mainen et al., 1999) effectively overcoming the depth limitations of single-photon absorption (1PA)-based setups (Vroom et al., 1999).

4.3.3 The fluorophore

The main prerequisite for 2PA, the simultaneous arrival of two photons, is achieved through generating highly concentrated excitation light. Based on their architecture, fluorophores may require different levels of spatiotemporal density of excitation light for successful 2PA, the quantification of which is expressed by the fluorophore molecular two-photon cross-section (σ_2) (Mutze et al., 2012). Its value is usually expressed in GM units (named after Maria Goeppert-Mayer, the Nobel laureate who discovered the two-photon absorption phenomenon (Göppert-Mayer, 1931)) where:

$$[\sigma_2] = 1 \text{ GM } = 10^{-50} cm^4 \text{s} \text{ (Drobizhev et al., 2011)}$$

4.3.4 The setup for two-photon laser-scanning microscopy

4.3.4.1 Generating high density of excitation light

The value of fluorophore σ_2 defines the properties of excitation light. In order to meet the set requirements, a two-photon laser-scanning microscope (2PLSM) needs to be capable of generating highly point-concentrated light. High spatial density can be achieved by a high NA objective (Denk et al., 1990) focusing the laser beam into a diffraction-limit point effectively limiting the excitation occurrence to a femtoliter volume (Dunn et al., 2000).

The power needed to nonlinearly excite the fluorophore molecule is very high (300 $PW.m^{-2}$ at the focal point) and would massively photodamage the sample if applied for longer periods of time. Therefore, the employment of pulsed lasers (such as the most commonly used Ti:Sapphire) capable of delivering long

wavelength light (650-1300 nm) of sufficient focal point intensity, while only exposing the sample to 100 fs pulses (τ_p) every 10 nanoseconds (corresponding to 100 MHz(f_p)), is necessary. For optimal 2PLSM, all of the elements in the excitation pathway (Fig. 7) are optimized for near-infrared (NIR) light (Helmchen and Denk, 2005).

4.3.4.2 xy deflection module – sample scanning

The xy deflection module, usually a pair of galvanometric mirrors, effectively scans the sample by deflecting the laser beam in *x,y* dimensions. For higher acquisition speed, an Acousto Optic Deflector (AOD) may replace one of the mirrors.

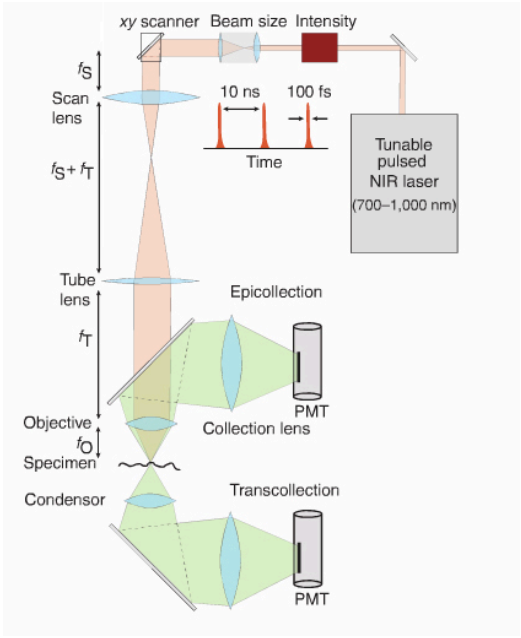

Fig. 7, A schema of a 2PLSM setup (Helmchen and Denk, 2005)

4.3.4.3 Fluorescence detection

The light emitted by the fluorophore can be detected either by transcollection or by epicollection. With thinner or transparent samples, and with samples where the fluorophore is excited using alternative non-linear techniques (second harmonic generation (SHG), coherent anti-Stokes Raman scattering (CARS)) the transcollection is more efficient (Helmchen and Denk, 2005). On the other hand, *in vivo*-physiology related imaging is mostly performed on thicker samples where light cannot traverse the whole sample, thus preferring epicollection (Oheim et al., 2001).

4.3.5 Light-matter interactions influencing image acquisition

4.3.5.1 Scattering

High energy density, needed for successful excitation of the fluorophore, is undesirably dissipated via scattering and absorption. Scattering is caused by interactions between light and matter, which lead to deviation of the photons from their original trajectory. The strength of scattering is described by the mean

free path (l_s), which defines the average distance between two scattering events and is strongly dependent on wavelength. However, for heterogeneous samples where the wavelength is comparable to the size of the studied structure is the scattering anisotropic (quantified by anisotropy parameter (g)) and the average distance between two scattering events is described by a transport mean free path (l_t):

$$lt = ls/(1-g)$$

The anisotropic factor (g) for brain tissue ($g_{brain} \approx 0.9$) (slightly higher for grey brain matter) rises with the wavelength (Yaroslavsky et al., 2002). According to the transport mean free path (l_t) definition, longer wavelength photons (with higher g) averagely travel longer distances without being scattered (remain ballistic) and allow deeper imaging (Oheim et al., 2001; Yaroslavsky et al., 2002; Helmchen and Denk, 2005). Also, wavelength-dependent Rayleigh scattering ($= \lambda^{-4}$), produced by single molecules and atoms, is lower for long wavelength light.

The emitted fluorescence falls into the visible part of spectrum, and its anisotropic parameter (g) is lower. Consequently, emitted fluorescence is subject to stronger scatter (Yaroslavsky et al., 2002) and possibly none of the emitted photons remain ballistic upon leaving the sample (Oheim et al., 2001). Since the focal spot in multiphoton microscopy is a near-diffraction limit point, all emitted fluorescence is relevant and whole-area detection may be used to capture every photon leaving the sample (Oheim et al., 2001).

4.3.5.2 Absorption of biological tissues in near-infrared (NIR)

Another argument in favor of the NIR excitation light is the existence of the NIR window, an interval of wavelengths with low absorption coefficients in biological tissue corresponding to light between 650 nm and 950 nm (covered by the tuning range of Ti:Sapphire lasers) (Smith et al., 2009).

Fig. 8 represents the tissue absorption spectra surrounding the NIR (first optical) window. The minimum represents the optical window itself, where low light absorption of biological tissue permits deeper imaging. The surrounding peaks represent light of either shorter wavelength, which is absorbed by hemoglobin, or longer wavelength light absorbed by water (and lipids).

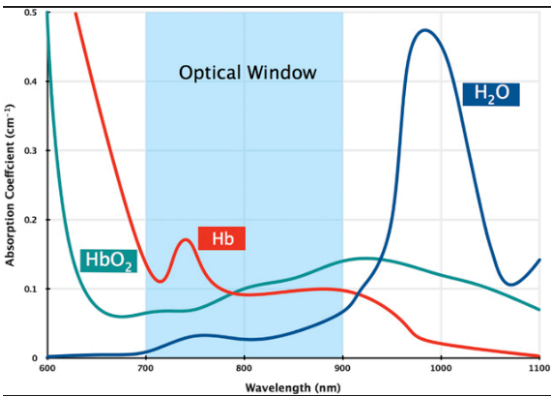

Fig. 8, Graphical representation of the absorption spectrum for biological tissue including the first optical window between the hemoglobin and water absorption peak (Phan and Bullen, 2010).

4.3.5.3 Laser beam dimensions

The numerical aperture (NA) of an objective is calculated for even illumination of the aperture. However, since the laser beam is Gaussian-shaped, the back aperture has to be slightly overfilled (Fig. 9a) under the conditions where $1/e$ of the laser beam diameter ≥ the back aperture diameter (Zipfel et al., 2003). The beam size "filling" the back aperture is often defined as the one where 86% of the power is transmitted through the objective. This corresponds to setting the beam width so that the point where the beam intensity falls to $1/e^2$ is at the edge of the aperture Fig. 9a.

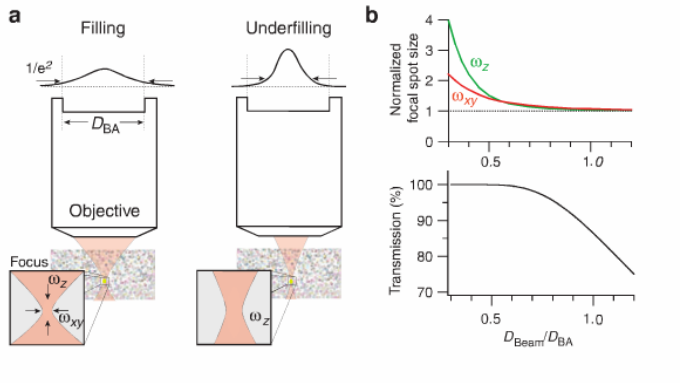

Fig. 9, *a)* The relation between laser beam size and aperture size and its impact on the focal spot dimensions. *b)* (top) Graphical representation of the relation between the "fill factor" (beam size/aperture size) and focal spot size, (bottom) Representation of the percentage of power throughput as a function of the "fill factor". (Helmchen and Denk, 2005)

4.3.5.4 Deep-imaging and its limitations

When imaging deeper layers of the sample, the ballistic fraction of the photons decreases exponentially (Beer-Lambert law). To retain sufficient fluorescence with growing depth, the number of excitation photons entering the sample needs to grow as well (Tsai and Kleinfeld, 2009). However, the laser power cannot be increased above a certain tissue-damaging threshold. Therefore, it is not the available laser power, which ultimately limits the maximal depth penetration (Wang et al., 2013).

The primary depth-limiting factor in 2PLSM is the growing scattering and absorption of excitation photons, which gradually leads to the loss of signal-to-background ratio (SBR) in deeper layers (Kobat et al., 2011). Low SBR results in insufficient contrast between the studied structure and the background, which prevents high-resolution image acquisition. Consequently, the maximal imaging depth for 800 nm excitation light corresponds to ~ 1 mm (Helmchen and Denk, 2005; Kobat et al., 2011).

Longer wavelength excitation (~1300 nm), which is subject to less scatter might be employed to acquire deeper images (>1 mm) (Kobat et al., 2011). However, 2PE under such conditions renders lower fluorescence since this part of the spectrum is dominated by water absorption (Fig. 8) (Horton et al., 2013).

4.3.6 Three-photon excitation as a tool for deeper imaging

The depth limitations restrict the use of *in vivo* 2PLSM imaging to the neocortex of the mouse brain (Horton et al., 2013). However, the existence of the second and third (plus suspected fourth) optical

window in biological tissue provides space for the application of even longer-wavelength excitation with deeper tissue penetration (Fig. 10) (Sordillo et al., 2014).

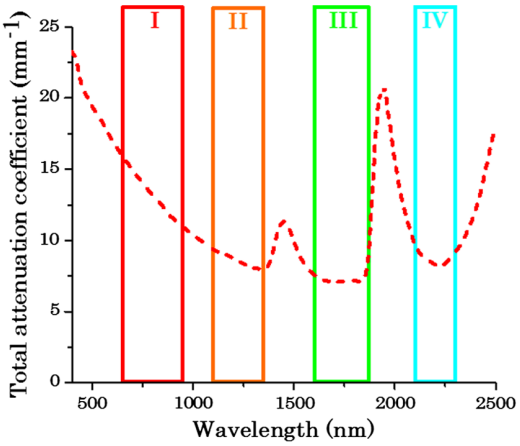

Fig. 10, Graphical representation of optical windows in different parts of the spectrum correlated with the attenuation coefficient (wavelengths with a high attenuation coefficient are less transparent) (Sordillo et al., 2014).

If the third optical window (~1700nm) (offering best scatter-absorption ratio) were to be targeted by two-photon excitation (2PE), the fluorophore excitation would occur in the NIR part of the spectrum. Moreover, the number of fluorophores capable of such absorption is still low (Horton et al., 2013).

The three-photon absorption (3PE) is a non-linear process where the excitation of the fluorophore molecule is reached by simultaneous absorption of three photons. The generated fluorescence is cubically dependent on the excitation intensity (compared to the quadratic relation in 2PE) (Xu et al., 1996). Moreover, the fluorescence decreases with distance from to focal plane (z) at $\approx 1/z^4$ compared to the $\approx 1/z^2$ of 2PE (Horton et al., 2013), which further eliminates the out-of-focus signal and generates superior SBR. Combined with the effect of scatter-proof excitation light (1700nm), the ballistic fraction arrives at greater depths, while generating more fluorescence, thus making 3PLSM capable of surpassing the depth limit set by 2PLSM while using regular fluorophores (Horton et al., 2013; Wang et al., 2013).

4.3.7 Resolution and its limitations for FM methods

The resolution achievable by an optical microscope can be theoretically defined by the Abbe diffraction limit (Abbe, 1873). It is a relation between the light wavelength (λ), the medium-specific refraction index (n) and the maximal half-angle of the objective light cone (θ), which defines the limit diameter (d) of the focal spot (Chereau et al., 2015) (eq2):

$$d = \frac{\lambda}{2\, n\, sin\, \theta}$$

The values of θ and n for an objective are constant. Therefore, an objective lens can be characterized by their value in the form of a dimensionless number, the numerical aperture (NA) (Eq. 3):

$$\mathrm{d} = \frac{\lambda}{2\, NA}$$

However, the diffraction-limit point is effectively represented by an approximately Gaussian-shaped point spread function (PSF), defined by additional factors, thus altering the theoretical value. The PSF of a confocal microscope is defined by the illumination light and by the detection pinhole (Eq. 4):

$$PSF = PSF_{illuminaton} \times PSF_{detection} \approx PSF^2_{illumination}$$

As for 2PLSM, the detection PSF is equal to the second power of the illumination PSF (Eq. 5):

$$PSF = PSF^2_{illumination}$$

In the case of LSCM, where the fluorophore is excited by 1PA, the excitation wavelength of commonly used fluorophores falls into the interval of [399nm (T-Sapphire[g]) – 590nm (mPlum[g])] (Shaner et al., 2005). The excitation light applied in 2PLSM is of significantly longer wavelength (NIR-800nm). Therefore, theoretically, LSCM should obtain resolution superior by a factor of 2 since the detection PSF is equal to second power of the illumination PSF and LSCM operates with wavelengths two times shorter. However, this would only be true if the confocal microscope had an infinitely small pinhole (Zipfel et al., 2003). Consequently, LSCM and 2PLSM are capable of achieving similar resolution (Helmchen and Denk, 2005) of around 200 nm (Gustafsson, 2000).

4.4 Light-sheet fluorescence microscopy

LSCM and 2PLSM acquire an image through point-illumination scanning. Consequently, the scanning speed of these methods is limited by the physical properties of the xy-deflection module. However, when analyzing neural activity, it is optimal to record from larger populations of cells simultaneously. This can be achieved by illuminating the sample from the side while the laser beam is focused into a micrometer thin "light-sheet" (Keller et al., 2008). Fluorescence is exclusively generated in the thin plane illuminated by the light-sheet, thus providing optical sectioning and a large field of view. A high-speed scanning light-sheet microscope, is capable of imaging the activity of the whole zebrafish brain every 1.3 s, while achieving cellular resolution in 80% of ~100 000 neurons (Ahrens et al., 2013).

4.5 Breaking the diffraction limit

The active zone of a synapse has a diameter of 300 nm (± 150 nm) (Ribrault et al., 2011). The 2PLSM and LSCM diffraction-limit resolution prevents these methods from effective imaging of such structures. The imaging of synapses or even single molecules is the domain of superresolution imaging microscopy.

4.5.1 Electron microscopy

Superresolution can be achieved through applying accelerated electrons of picometer wavelength instead of photons, for image acquisition in electron microscopy. The extremely short wavelength results in

high resolution, which enables imaging of very small structures such as recombining DNA (Griffith et al., 1999). The achievable resolution is demonstrated by an example, where spacing of less than 50 pm has been resolved using transmission electron microscopy (Erni et al., 2009)

In terms of neurological significance, electron microscopy has been used to map the connectome of *C.elegans* (White et al., 1986), and is being used to map other model organisms as well. However, the amount of data generated by such mapping makes it currently impossible to apply this method to higher organisms. Therefore, while its benefit in the field of neurophysiology is significant, it is also limited.

4.5.2 Recent superresolution methods

The diffraction limit can also be broken by more recent methods. These, among else, include the following:

Total internal reflection fluorescence (TIRF), a near-field method used for imaging cell surfaces with high axial resolution where excitation light reaches only 100-200 nm into the sample (Schermelleh et al., 2010).

Structured illumination microscopy (SIM), a wide-field method where illumination of the sample by stripe-shaped sinusoidal patterns interferes with the emission of studied structures, thus surpassing the diffraction limited resolution by a factor of two (Schermelleh et al., 2010).

Stochastic optical reconstruction microscopy (STORM) and photo-activated localization microscopy (PALM) are two closely related wide-field methods, which break the diffraction limit by using the fact that a single fluorophore molecule can be localized with nanometer resolution if not surrounded closely by other emitters (Rust et al., 2006). Switchable cyanine dyes in STORM, or genetically encoded switchable fluorophores in PALM present in the sample can be reversibly controlled by the applied laser wavelength. Only a fraction of the fluorophores emits fluorescence during a light cycle and therefore single points can be resolved with better resolution (up to 20 nm) (Rust et al., 2006).

Stimulated-Emission-Depletion fluorescence microscopy (STED) possesses an excitation light pathway virtually identical to a regular confocal microscope. In addition, a second laser divided into two beams acts as a quencher by inducing de-excitation around the focal spot. Therefore, it effectively reduces the diameter of the point where excitation leads to the emission of fluorescence (Hell and Wichmann, 1994). Today, instead of two laser beams, the quenching laser has a shape of a doughnut (Chereau et al., 2015). The de-excitation of the fluorophore is realized through stimulated emission of a longer wavelength photon by the STED laser. Because of the wavelength difference between the standard fluorescence emission and the stimulated emission, it is possible to filter out the latter (Chereau et al., 2015). The resolution obtained by STED imaging is 4.5x higher than of regular confocal microscopy (Hell and Wichmann, 1994). For illustration, a fluorophore excitable by 400 nm can be imaged by a NA=1.4 objective at a resolution of 35 nm (Hell and Wichmann, 1994).

In neurosciences, STED is optimal for subcellular imaging such as studying dendritic spine plasticity in brain slices (Nagerl et al., 2008). However, recent publications showed its applicability even *in vivo* in cortical neurons of living mice (Berning et al., 2012).

5 Reporting neuronal activity

High-resolution imaging tools such as 2PLSM combined with modern fluorophores have significantly increased the scale in which neural activity can be observed. Hopefully, these new methods will provide more insight into the, yet undiscovered, general principles of how information is coded and processed by neural tissue.

5.1 Definition of neural activity

Neural activity carries information in the form of a change in electrical behavior of the neuron membrane, the action potential (AP). An AP consists of a rapid depolarization (Na^+ influx) followed by a brief hyperpolarization (K^+ outflow) (Hodgkin and Huxley, 1952). Moreover, an AP is also accompanied by the rise of intracellular calcium (Ca^{2+}) concentration (Baker et al., 1971) mediated by voltage-gated Ca^{2+} channels (Magee and Johnston, 1995) and Ca^{2+}induced Ca^{2+} release from intracellular deposits (Llano et al., 1994). Calcium is an important second messenger and it has a significant role in modulating cellular physiology (Berridge, 1998) such as the control of neuronal excitability (Berridge, 1998) or neurotransmitter release (Uchitel et al., 1992).

5.2 Electrophysiology

A high-resolution representation of neural activity can be achieved through directly monitoring electrical properties of single neurons via electrodes.

5.2.1 Extracellular recording

Extracellular electrical recording of neural spikes (corresponding to single APs) has been, classically, the dominant technique in *in vivo* neurophysiology (Chorev et al., 2009; Lutcke and Helmchen, 2011). For example, it has been used to determine the receptive fields of single neurons in cat striate cortex (Hubel and Wiesel, 1959). Moreover, if multiple electrodes are used (tetrodes or multi-shank silicon probes), simultaneous recording from effectively up to 100 neurons is possible via triangulation and spike sorting algorithms (Buzsaki, 2004). The main limitations of extracellular recording lie within insufficient identification of recorded neurons (Buzsaki, 2004; Chorev et al., 2009). Also, this technique does not provide the means to manipulate with the neuron (Chorev et al., 2009) and may lead to ignoring silent neurons.

On the other hand, juxtacellular electrical recording is capable of manipulating with, and labeling (biocytin) of single neurons via electroporation (Chorev et al., 2009). Furthermore, it is preferable over intracellular recording in terms of tissue damage. However, due to specific micropipette positioning and its

proximity to the cell, *in vivo* juxtacellular recording is restricted to a few cells, while there is a hazard of damaging them (Chorev et al., 2009).

5.2.2 Intracellular recording

Intracellular recordings provide the most detailed insight into the electrical activity of single neurons. Aside from the possibility to stimulate and label neurons, intracellular recordings also detect sub-threshold events such as synaptic potentials (Chorev et al., 2009). For example, whole-cell patch-clamp recordings of barrel cortex neurons were conducted to observe the dynamics of neural spikes during whisker-related behavior of awake mice (Crochet and Petersen, 2006). However, in awake studies, the rate of successful recordings is rather low, while the duration of the recording is limited to ~1 hour (Chorev et al., 2009).

5.3 Optophysiology

Recordings of single cells cannot sufficiently uncover the function of multicellular neural networks (Knopfel et al., 2006). Small-molecule fluorescent dyes or fluorescent proteins capable of detecting the changes associated with an AP, significantly extend the scale of possible neural activity recordings. If imaged by high-resolution fluorescence microscopes, fluorescent probes exhibit alterations in emitted fluorescence coupled with the binding of Ca^{2+} ions or changes in membrane voltage.

5.3.1 Fluorescence reporting

Fluorescent neural activity reporters include small organic fluorescent dyes and genetically encoded fluorescent proteins. These share similar general architecture and are dividable into two groups based on the number of employed fluorophores. In single-fluorophore reporters, binding of the ligand results in a conformational change of the sensor, which leads to altered fluorescence. In the case of Förster resonance energy transfer (FRET) reporters, two fluorophores are present in a single molecule. One, instead of fluorescence emission, transfers its energy to the other via a dipole-dipole interaction (Dunn et al., 1994). The binding of the ligand induces conformational changes resulting in reduced distance between the fluorophores. The resulting increase in energy transfer efficiency leads to a change in the ratio of the respective fluorescence contributions, which can be measured (Smedemark-Margulies and Trapani, 2013). Ratiometric fluorescence imaging allows for quantitative fluorescence microscopy (Dunn et al., 1994), since such reporters can be precisely calibrated. Moreover, it minimizes the effect of photobleaching, uneven dye loading, motion artifacts and leakage, all of which are common problems of single fluorophore reporter dyes (Paredes et al., 2008).

5.3.2 Small organic dyes

In the past, cellular morphology and physiology has been fluorescently imaged mostly using synthetic organic dyes (Lutcke and Helmchen, 2011). These include widely used molecules such as DAPI used to stain nucleic acids since 1970s (Kapuscinski, 1995), or others based on fluorescein or rhodamine

(Minta et al., 1989). The major advantages of synthetic dyes over protein probes lie within the ease of their application, commercial availability and large variety of different affinities (Paredes et al., 2008). Moreover, synthetic reporters often outperform protein probes in binding kinetics and signal-to-noise ratio (SNR) (Hendel et al., 2008). However, high concentration of organic dyes may negatively interfere with physiological functions of cells (Paredes et al., 2008). Furthermore, organic dye targeting into specific cell populations is very limited.

5.3.2.1 Voltage sensitive dyes (VSDs)

The change in membrane potential was the first AP-associated phenomenon targeted by fluorescent probes. First fluorescent dyes such as 8-Anilinonaphthalene-1-sulfonic acid (ANS) (Tasaki et al., 1968) did not yet generate sufficient SNR for neural activity reporting (Cohen et al., 1978). However, inspired by these, merocyanine-rhodanine dyes were synthetized with the SNR as high as 100:1 (Ross et al., 1977). VSDs are normally membrane-bound molecules, which exhibit a fast change in the absorption during a change in membrane potential (Fig. 11).

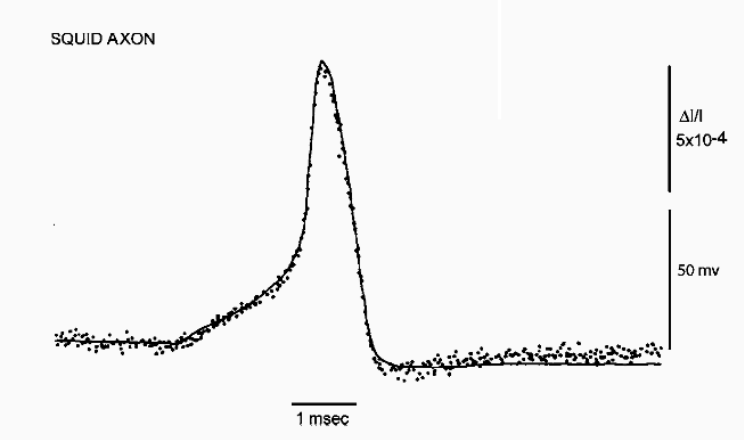

Fig. 11, Simultaneous recording of the change in absorption of a merocyanine dye (dotted) and the electrophysiological recording of an AP (line) (Baker et al., 2005)

Currently used VSDs such as RH1691 have improved sensitivity and staining efficiency (Lutcke and Helmchen, 2011). However, they are not capable of reporting at cellular resolution and are, therefore, limited to indication of neural activity of neural populations. For example the activity of rat barrel cortex columns during whisker stimulation (Petersen et al., 2003). The molecular mechanisms underlying the reporting of different VSDs include electrochromism, potential sensitive monomer-dimer equilibrium and dipole rotation (Baker et al., 2005). Since VSDs are lipophilic, cells can be placed directly into the VSD containing solution during *in vitro* studies (Berger et al., 2007). For *in vivo* studies, the VSD dissolved in artificial cerebrospinal fluid (ACSF) is directly applied to *dura mater* above the imaged brain region (Lippert et al., 2007).

The major advantages of VSDs include high SNR and capacity to detecting sub-threshold activity. On the other hand, VSDs cannot report at the cellular resolution *in vivo* and are more suitable for large scale activity tracking such as the spread of tactile sensory information to the motor cortex (Ferezou et al., 2007).

5.3.2.2 Calcium indicators

Synthetic indicator-based fluorescent reporting on AP-evoked Ca^{2+} transients delivers a good representation of neuronal supra-threshold activity (Lutcke and Helmchen, 2011), providing single-cell and single-AP resolution *in vivo* (Kerr et al., 2005; Grewe et al., 2010). Synthetic calcium indicators are usually based on a highly selective calcium chelator such as EGTA or its derivative BAPTA, which is covalently linked to a fluorescent reporter (Thomas et al., 2000).

As for the mode of delivery, firstly, small-molecule calcium reporters can be delivered into the cell as salts via microinjection, patch-pitpette or in liposomes (Paredes et al., 2008). However, these tend to compartmentalize which is negative for calcium imaging. This problem can be solved by the application of their dextran conjugates (Paredes et al., 2008). Nevertheless, these are also membrane impermeable and normally require invasive cell-loading (Paredes et al., 2008) such as cilia removal by a nonionic detergent ,such as Triton X100 (Friedrich and Korsching, 1997), as when imaging olfactory bulb neurons by Calcium green dextran (Wachowiak and Cohen, 2001). Finally, the most widely used technique for *in vivo* calcium probe delivery is the multi-cell bolus loading (MCBL) (Stosiek et al., 2003). It is based on local pressure ejection of membrane-permeant acetoxymethyl (AM) esters of calcium indicators into the tissue (Stosiek et al., 2003). Such engineered probes traverse the plasma membrane into the cytosol, where the AM group is cleaved of by endogenous esterases, thus trapping the rest of the molecule inside (Grynkiewicz et al., 1985). As little as 400 fl of dye-containing solution is able to stain a spherical region with a diameter of 300 μm (Stosiek et al., 2003).

Among the single-fluorophore calcium dyes, the best properties were attributed to fluo-3 over Oregon Green 488 BAPTA-1 (OGB-1) (Thomas et al., 2000). However, since OGB-1 (Fig. 12) is more suitable for 2PLSM (Paredes et al., 2008), it is the most widely used fluorescein-like calcium probe in *in vivo* calcium imaging.

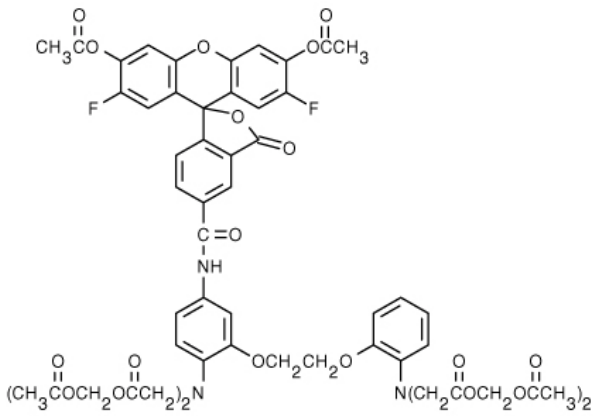

Fig. 12, The chemical structure of OGB-1 AM, the most widely used synthetic calcium indicator prepared for MCLB.

Among the ratiometric dyes fura-2 (Grynkiewicz et al., 1985) has been most popular for quantitative measurements, although it is non-ratiometric in 2PE (Paredes et al., 2008), while Indo-1 (Grynkiewicz et al., 1985) remains ratiometric in 3PE (Paredes et al., 2008). The main disadvantage of synthetic calcium dyes is the absence of targeting, artificial buffering of calcium and also leakage after longer time periods (Thomas et al., 2000; Paredes et al., 2008), with low chance of successful relabeling (Lutcke and Helmchen, 2011). Nevertheless, synthetic Ca^{2+} reporters have historically outperformed protein probes in Ca^{2+} binding kinetics and SNR (Hendel et al., 2008).

5.3.3 Protein-based indicators of neuronal activity

Simultaneous recording of specific neuronal populations is essential for the understanding of fundamental principles of neural network functioning. Genetically encoded protein probes are composed entirely of amino acids and they are independent of cofactors (as opposed to synthetic dyes). Therefore, if their coding sequences are integrated into the genome of a model organism, the expression of the probe is mediated *in situ* by cells themselves and does not require loading (Mank and Griesbeck, 2008). Furthermore, the spatiotemporal aspects of protein expression can be controlled by genetic engineering methods, described in previous chapters. In addition, properties such as the dynamic range of protein reporters may be adjusted by targeted mutation to better fit the requirements of the experiment (Baker et al., 2008).

5.3.3.1 General architecture of protein indicators

The principle of expressing genetically encoded indicators with cell-type specificity, was first proposed in the case of a bioluminescent calcium indicator, aqueorin (Knopfel et al., 2006). However, due to its requirement of a cofactor and limited light output, it proved suboptimal for brain imaging (Stables et al., 2000; Knopfel et al., 2006; Mank and Griesbeck, 2008).

Optimal probe properties were finally achieved by engineering reporters based on the Green Fluorescent Protein (GFP) (Heim et al., 1995; Tsien, 1998), exhibiting the unique trait of autocatalytic fluorescence (Mank and Griesbeck, 2008). A single XFP (a GFP mutant of a different color), or a FRET pair is fused to a transducer protein sensitive to specific neural activity-evoked physiological changes in parameters such as intracellular calcium concentration or membrane potential (Knopfel et al., 2006). A conformational change of the biosensor induced by the transducer protein in the event of neural activity, results in detectable change of fluorescence (Knopfel et al., 2003).

5.3.3.2 Voltage sensitive protein reporters

The first generation of genetically encoded voltage indicators (GEVIs) has been engineered by fusing a GFP-based reporter (or a FRET pair) to various sites of a voltage-gated ion channel (or a part of it),

with subsequent screening for functioning probes (Knopfel et al., 2003; Baker et al., 2008). This approach resulted in the creation of three different prototypes: FlaSh, based on the *D. melanogaster* K^+ Shaker channel (Siegel and Isacoff, 1997), SPARC, exploiting the skeletal muscle Na^+ channel (Ataka and Pieribone, 2002) and VSFP1, using only the voltage-dependent S4 domain of the Kv2.1 channel (Knopfel et al., 2003). The main limitation of the first generation voltage sensors has been mostly poor plasma membrane targeting in mammalian cells combined with large background signal (Dimitrov et al., 2007).

The second generation of voltage-sensitive protein reporters has been focused on "self-contained" voltage-sensor domains (Baker et al., 2008). These do not form multi-subunit complexes such as ion channels, thus modulating the negative effect fluorescent tags might have had on the first generation reporter folding (Baker et al., 2008). A non-ion channel protein (Ci-VSP) containing a phosphoinositide phosphatase and a self-contained voltage-sensing domain (homologous to S1-S4 domains of voltage-gated channels) was discovered in an ascidian *Ciona intestinalis* (Murata et al., 2005). A FRET pair (CFP/YFP) was fused to the voltage-sensing domain of Ci-VSP, replacing the phosphatase domain (Dimitrov et al., 2007) resulting in VSFP2(A-D). Additional refinement led to the development of ArcLight, the most advanced Ci-VSP-based GEVI to date, with superior SNR, capable of single-trial optical electrophysiology (Cao et al., 2013).

However, Ci-VSP-based GEVIs suffer from weak dynamic responses, which prevent these sensors from reliably imaging fast-spiking neurons (Gong et al., 2014). Therefore, the next generation of GEVIs includes changes in protein architecture aimed at solving these issues. The Accelerated Sensor of APs (ASAP1) includes a single circularly permuted GFP attached to the extracellular S3-S4 loop of the VSD (Fig. 13) (originating from a chicken phosphatase), which ultimately enables higher brightness and faster kinetics (St-Pierre et al., 2014). Comparable values were reached creating a class of FRET-opsin sensors where Mac rhodopsin serves as both VSD and FRET acceptor, and mCitrine serves as FRET donor (MacQ-mCitrine) (Gong et al., 2014). These third generation GEVIs have now approached the level of single-cell *in vivo* membrane-potential recordings, but have not yet surpassed the reliability of calcium indicators (Gong et al., 2014).

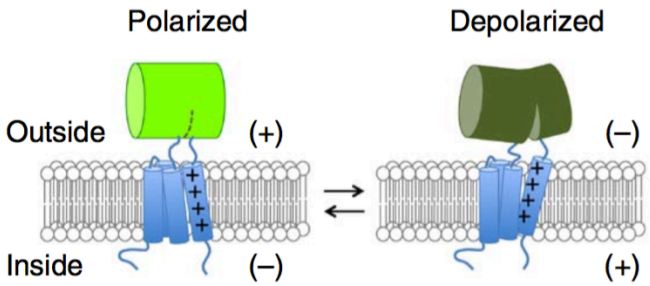

Fig. 13, Schematic representation of the mechanism of neural reporting by ASAP1, which includes a cpXFP fused to the extracellular part of a VSD (St-Pierre et al., 2014).

Among the advantages, GEVIs report on sub-threshold neural activity including inhibitory synaptic potentials at a very high temporal resolution (Lutcke and Helmchen, 2011). However, some GEVIs may change the physiological properties of the membranes by increasing their capacitance, which may result in altered subthreshold and spiking properties (Baker et al., 2008).

5.3.3.3 Genetically encoded calcium indicators (GECIs)

Apart from the fluorescent tag common for most of the genetically encoded protein indicators (XFPs/FRET pair), GECIs include a transducer domain capable of protein-based Ca^{2+} chelation (Mank and Griesbeck, 2008). The EF hand domain was selected among the other considered Ca^{2+}-binding domains to serve as a transducer in GECIs since it binds one calcium ion with constant kinetics (Mank and Griesbeck, 2008). The calcium ion is bound in the loop section of the helix-loop-helix motif first described in parvalbumin (Kretsinger and Nockolds, 1973). EF-hand domains always occur in pairs with cooperativity in Ca^{2+} binding (Grabarek, 2006), which in regulatory proteins, such as calmodulin or troponin C, results in conformational changes.

5.3.3.3.1 FRET sensors

The first GECI, cameleon-1, was constructed exploiting the conformational change of calmodulin (CaM) coupled with a change in the fluorescence ratio of a FRET pair (Miyawaki et al., 1997). Apart from a XFP, CaM is also fused to a calmodulin-binding peptide (M13) from the myosin light chain kinase (Ikura et al., 1992), also bearing a fluorescent tag (Fig. 15). Binding of a calcium ion results in close interaction between CaM and M13, which subsequently brings the two XFPs closer together, thus altering the fluorescence ratio of the FRET pair (Miyawaki et al., 1997). The employment of M13 was motivated by the aim to increase fluorescence and by the need to interfere with possible binding of endogenous CaM-binding proteins (Mank and Griesbeck, 2008).

Further development led to Yellow cameleon (YC), later refined into YC2.60, or D3cpVenus and YC3.60, which use circularly permuted variants of XFPs (Baird et al., 1999) with higher SNR (Nagai et al., 2004). These probes, however, still proved not sensitive enough for *in vivo* studies (Horikawa et al., 2010). Further extension of the linker between CaM and M13 of YC2.60 led to the creation of the ultrasensitive probe YC-Nano. YC-Nano proved capable of imaging small perturbation of Ca^{2+} concentration (10 -100 nM) *in vivo* by 2PLSM (Horikawa et al., 2010).

However, native CaM (playing a significant role in cell signaling) has been known to interact with CaM-based GECIs, thus interfering with their reporting (Nakai et al., 2001). Apart from the alteration of CaM and M13 (Palmer et al., 2006), this problem may be addressed by using a different EF-hand-containing protein for Ca^{2+} chelation such as Troponin C (TnC) (Mank and Griesbeck, 2008). The role of muscle TnC, which is not found free in the cytosol, is exclusive to muscle contraction regulation (as a part of a complex) and therefore TnC-based reporters are not subject to endogenous protein binding (Mank and Griesbeck, 2008), which minimalizes their impact on cell physiology (Mank et al., 2006). TnC-based FRET

sensors were constructed, similarly to their CaM-based counterparts, by sandwiching the TnC construct between two XFPs, such as CFP and Citrine in the first sensor TN-L15 (Heim and Griesbeck, 2004). Subsequently, versions with enhanced signal strength such as TN-XL (Mank et al., 2006) or further improved TN-XXL (Mank et al., 2008) were engineered. Twitch sensors represent the most recent development in TnC-based FRET sensors. They were designed on the basis of TN-XXL, with the aim to reduce the Ca^{2+}-sensitive domain to a minimum, since originally these sensors bind up to 4 calcium ions per molecule (Thestrup et al., 2014). As a result a minimal calcium-binding motif was identified (C-terminal domain of TnC), binding only 1 or 2 ions per molecule, thus reducing the calcium buffering and the subsequent effect on cell physiology (Thestrup et al., 2014). Twitch sensors have proven useful in *in vivo* neural activity reporting, while outperforming the CaM-based FRET sensor, YC3,60 (Thestrup et al., 2014)

5.3.3.3.2 Single-fluorophore

As opposed to FRET sensors, single-fluorophore GECIs report on calcium transients by altering the fluorescence of a single XFP. The fusing of GFP (or its mutated forms) to transducer proteins has been made possible by the emergence of its circularly permuted variants (cpXFPs) (Baird et al., 1999), which have altered N and C termini locations. Subsequent successful fusion of a cpEYFP to the C terminus of M13 and to the N terminus of CaM has yielded a fluorescent Ca^{2+}-sensitive protein pericam (Nagai et al., 2001). The most popular single-fluorophore GECI (Mank and Griesbeck, 2008), GCaMP, was created analogously using a cpEGFP fluorescent tag instead of its yellow mutation (Fig. 15) (Nakai et al., 2001).

Further targeted improvements of GCaMP were made possible by the description of its structure and molecular mechanisms underlying fluorescence generation (Akerboom et al., 2009). Subsequent structure-guided mutagenesis and semi-rational library screening resulted in versions such as GCaMP3 with improved parameters including SNR, photostability and kinetics. However, GCaMP3 is not capable of resolving single APs during *in vivo* experiments and further refinement (same principle as before) was required to obtain higher sensitivity found progressively in GCaMP5 (Fig. 14) (Akerboom et al., 2012) and most recently GCaMP6, which has become the first GECI to reach single AP resolution (Chen et al., 2013).

In order to include the specific properties of neuronal calcium signaling, the development of GCaMP6 included screening of the generated mutants in neurons (Chen et al., 2013) rather than in *E.coli* (used previously (Akerboom et al., 2012)). Multiple rounds of targeted mutagenesis resulted in three GCaMP6 variants (s-slow, m-medium and f-fast). The most sensitive variant, GCaMP6s, produces fluorescence signals more than 10 times larger than GCaMP3, while the fastest variant, GCaMP6f, achieved unprecedented sensitivity (in terms of GECI) for single APs, comparable to OGB-1 (Chen et al., 2013) (Fig. 14). Moreover, GCaMP6 sensors are capable of detecting more active neurons than other GECIs or OGB-1. In addition, experiments coupled with electrophysiological recordings have proven that GCaMP6 sensors are able to resolve single spikes at high detection rates (Chen et al., 2013). Finally, long-term experiments including multiple imaging sessions separated by months suggest that the expression of GCaMP6 does not interfere with the function of neural circuits (Chen et al., 2013).

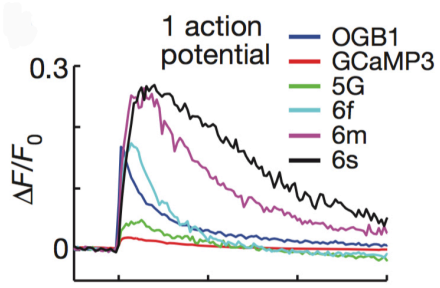

Fig. 14, Average responses to one action potential for different variants of GCaMP- (6f, 6M, 6S, 5G, 3) and OGB-1 (Chen et al., 2013).

The novel advancements transformed GECIs into the most widely used method for *in vivo* neural activity reporting, while modern GEVIs are well-suited to complement calcium imaging by adding more temporal precision to electrical events beyond single spikes (Gong et al., 2014).

5.3.3.4 FRET vs. single-fluorophore reporters

The choice of a specific sensor is strictly dependent on the nature of the experiment. The FRET-based sensors are universally better for quantification studies, which may be advantageous during long-term functional imaging (Thestrup et al., 2014), or when expecting significant background noise (Smedemark-Margulies and Trapani, 2013). Also, FRET-based sensors generate higher resting signal, which enables easier identification of inactive cells, as well as the distinction between resting and continually active neurons (Thestrup et al., 2014). On the other hand, single-fluorophore sensors exhibit higher photostability and better SNR (Nakai et al., 2001) with stronger signal and faster kinetics (Tian et al., 2009), which enables modern sensors such as GCaMP6 to detect single APs in large scale with high reliability.

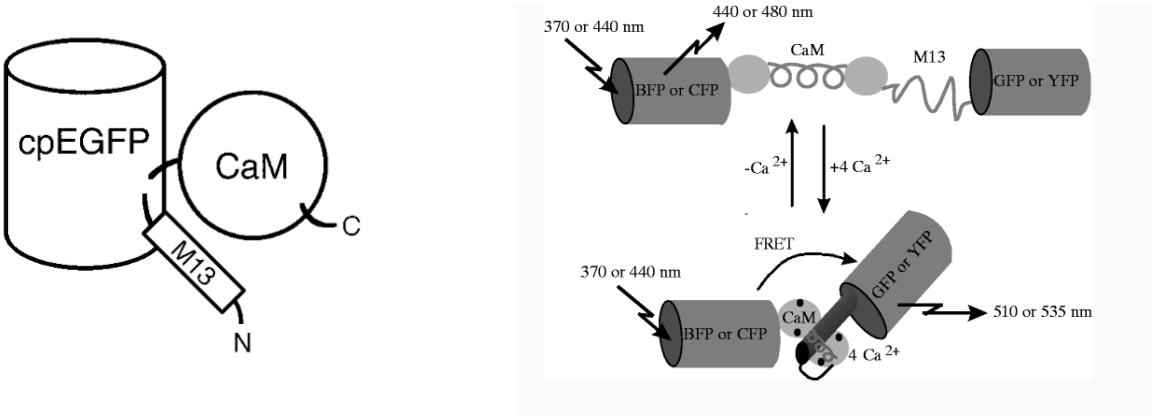

Fig. 15, *Left:* A schematic representation of the GCaMP family of calcium probes. The use of cpEGFP has enabled the fusion of both CaM and M13 to a signle cpXFP (Nakai et al., 2001). *Right*: A graphic representation of the mode of action of FRET CaM-based calcium sensors (cameleon-1) (Miyawaki et al., 1997).

5.3.3.5 Synthetic dyes vs. protein-based sensors

Synthetic dyes lack the cell-type-specifity or large-scale application possible by protein indicators. However, their ease of use, high SNR and the fact that they do not require valuable transgenic models, makes them continuously relevant in acute *in vivo* experiments.

5.3.3.6 Optophysiology vs. electrophysiology

Recordings based on neural activity-dependent changes in fluorescence should always be supported by electrophysiological recordings in order to be completely relevant (Gong et al., 2014). This is due to the fact that electrophysiological techniques are capable of recording neural activity with high temporal resolution and AP-detection reliability much greater compared to synthetic or protein-based probes. However, large-scale cell-type-specific recordings of neural networks *in vivo* are technically unfeasible by electrophysiological methods and remain an exclusive domain of optophysiology. Therefore, it is safe to say that optophysiological and electrophysiological methods are, in many aspects, complementary.

5.4 Review of selected methods

Recently, a number of new techniques have further extended the applicability of the mentioned imaging methods. Some of these are reviewed in the following paragraphs.

5.4.1 Cranial window technique

The application of 2PLSM in chronic *in vivo* brain experiments required a method capable of eliminating the natural optical barrier represented by the skull. The cranial window was originally developed as a tool for studying angiogenesis of transplanted tumors in mice models (Yuan et al., 1994), while being later repurposed for neurophysiology, first during studies concerning long-term synaptic plasticity using 2PLSM (Trachtenberg et al., 2002). The chronic cranial window is created by carefully drilling the skull with a small-sized burr-tip drill, while applying cold saline in order to minimize thermal damage of the underlying tissue (Yuan et al., 1994). Upon removing a region of the skull, the exposed dura is usually covered with agarose, coverslipped and sealed by dental acrylic. After 7-10 days of recovery, the animal is ready for imaging (Trachtenberg et al., 2002) and does not display any behavioral deficits. Besides experiments under anesthesia, such mice may also be used for cortical calcium imaging under diverse behavioral conditions (Dombeck et al., 2007).

Another related method, the transcrianial imaging, does not require craniotomy and therefore represents a less invasive alternative for cortical imaging. In some cases, it has surprisingly rendered different results compared to craniotomy-based experiments (Wilt et al., 2009). Transcranial two-photon imaging includes thinning of the skull with a high-speed drill (including frequent cooling with cold sterile solution) to a thickness of ~ 50μm (Grutzendler et al., 2002). For example, this technique was used for calcium imaging of the auditory cortex of a unanesthethized GCaMP3-expressing mouse (Issa et al., 2014).

However, repeated skull thinning results in opaqueness of the skull due to bone regrowth, which limits the number of screenings (Wilt et al., 2009).

5.4.2 Microendoscopy

Whole-brain anatomy and physiology can be studied by non-invasive methods such as PET (positron emission tomography) or MRI (magnetic resonance imaging) (Jacobs and Cherry, 2001). However, the achievable resolution is significantly lower in comparison to fluorescence microscopy (Levene et al., 2004). On the other hand, advanced FM methods, such as 2- or 3PLSM, are capable of imaging structures only in the order of one millimeter from the surface, (corresponding to mouse neocortex) (Horton et al., 2013).

To overcome this limitation, invasive microendoscopes, which serve as an "extension" of the original setup, can be introduced into the sample tissue. The microendoscope is comprised of a gradient-index (GRIN) lens triplet including an objective lens, a relay lens and a coupling lens (Fig. 16b) (Jung and Schnitzer, 2003). These GRIN triplets are capable of translating an excitation beam focused at the coupling lens, so that it is focused approximately the same way by the objective lens into a focal plane within the sample (Fig. 16a) (Jung and Schnitzer, 2003). Today, microendoscopy is performed using both two-photon (laser-scanning) and one-photon (laser-scanning, or wide-field) excitation including miniaturized setups (Fig. 16c) capable of long-term calcium imaging of hippocampal CA1 neurons in behaving, freely-moving mice (Ziv et al., 2013)

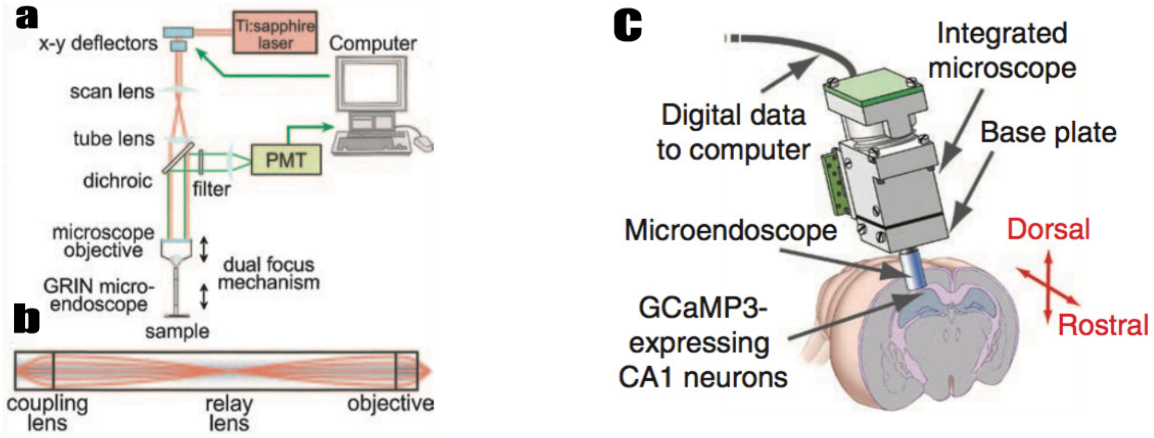

Fig. 16, *a*: a schematic representation of a multiphoton endoscopy setup, *b*: a representation of how the focused laser beam is relayed by a GRIN triplet, *c*: a miniaturized portable setup enabling calcium imaging of deep brain regions (Jung and Schnitzer, 2003; Ziv et al., 2013).

The achievable resolution of multiphoton GRIN-based microendoscopy is around 850 nm (Jung et al., 2004), while the depth reachable by the probe is in the order of centimeters (Levene et al., 2004). The price for the recording from almost any depth is the fact that the insertion of the microendoscope

traumatizes the above lying tissue. However, such tradeoff is often acceptable since the diameters of the endoscopes range from 350 to 1000μm.

5.4.3 Two-photon Targeted Patching (TPTP)

Classical electrophysiological recordings provide data with superior temporal resolution. However, the inability to target specific neurons has been a significant limitation of the application of electrophysiology *in vivo* (Margrie et al., 2003). This problem may be solved by genetically labeling target neurons with fluorescent probes, which then mark the cells of interest for optically targeted whole-cell recordings. This technique, called two-photon targeted patching (TPTP), has allowed the identification and whole-cell recordings of any type of cortical cell in a living experimental animal (Margrie et al., 2003).

6 Modulation of neural activity; Optogenetics

As proposed by Francis Crick (Crick, 1979), the key to profound understanding of how the brain functions, may not lie within the outside analysis of natural or unnatural behavior, but in the capacity to precisely interfere at multiple levels, most notably cellular and molecular (Crick, 1999). Electrophysiology is capable of achieving high temporal precision in electrical manipulation, however, with poor cell-specificity. Conversely, genetic and pharmacological tools are able to target specific cell-types, although not with sufficient temporal resolution (Fenno et al., 2011).

The lack of methods with sufficient cellular and temporal resolution has inspired the search for new approaches. The combination of optical and genetic methods, optogenetics, possesses optimal properties since it allows non-invasive high-resolution manipulation (microseconds and micrometers) upon minimal interference with cellular physiology.

6.1 Multi-component tools

First methods capable of light-driven control over cellular physiology relied on multi-component tools. In the beginning, these approaches aimed for direct optical control over the loss, or gain of function of specific proteins or ligands.

6.1.1 Chromophore-assisted laser inactivation (CALI)

The chromophore-assisted laser inactivation of a protein uses specific antibodies or ligands conjugated with malachite green, to denature the bound protein if irradiated by a specific wavelength (Jay, 1988). This technique was, for example, used for studying stage-specificity of the segments-polarity protein Patched during *D. melanogaster* embryogenesis (Schmucker et al., 1994).

6.1.2 Uncaging

Another multi-component method involves the conditional inactivation of a molecule active in cellular physiology by adding a photolabile group, also termed “caging”. This blocking group is degraded upon irradiation by a specific wavelength, thus freeing, or “uncaging” an active agonist (Mayer and Heckel, 2006). Neurophysiology has adapted this method for spatially conserved light-activation of caged

neurotransmitter receptor agonists, mostly glutamate hence its capacity to activate most of the mammalian brain neurons, thus provoking neural activity with high specificity (Callaway and Katz, 1993). Moreover, 2PLSM has now allowed the photolysis of caged glutamate *in vivo*, thus further expanding the tools needed to study synaptic properties, for which this method proved optimal (Noguchi et al., 2011).

To further improve cell-type specificity, heterologous receptors responding to non-neurotransmitter ligands can be genetically encoded into the targeted neuronal type, thus adding a different level of control over the neuron stimulation (Zemelman et al., 2003). The nociceptive vanilloid (TRPV1) and menthol (TRPM8) ionotropic receptors present ideal heterologous receptors for neurons of the mammalian brain. They are naturally expressed exclusively in the peripheral nervous system, and their agonists capsaicin or menthol do not act as neurotransmitters while they contain acceptor sites for a photoremovable caging group (Zemelman et al., 2003). For experiments in *D. melanogaster,* nociceptive channels were replaced with a purinergic $P2X_2$ channel due to the retention of TRPV1 in ER (endoplasmic reticulum) of insect cells. During these experiments, it was shown that stimulation of dopaminergic neurons triggers changes in locomotion along with inducing exploratory behavior (Lima and Miesenbock, 2005)

6.1.3 Photoswitchable receptors

Another approach to achieving remote control over genetically specified cell-types is to covalently bond an ion channel to a "tethered" agonist through a photoisomerizable azobenzene linker. Light-induced photoisomerization of the linker optimally manipulates with the position of the ligand in relation to its binding site, thus activating the channel, as in the LiGluR (light-activated ionotropic glutamate receptor) (Volgraf et al., 2006). The LiGluR can be "turned on" by a light pulse inducing the *cis*- transition (380 nm) and remains in this state even without photostimulation up until the *trans*- state is provoked by a light pulse of 500 nm (Fig. 17) (Volgraf et al., 2006). This allows for long depolarizations without extensive exposure to light (Szobota et al., 2007). Moreover, control over the neuronal activity achieved through photoswitching allows reliable recreation of subthreshold activity (Szobota et al., 2007). It has been shown that the activation of LiGluR in specific neurons of transgenic zebrafish may result in a change of behavior such as blocking of the escape reflex, while not being toxic to the animal (Szobota et al., 2007).

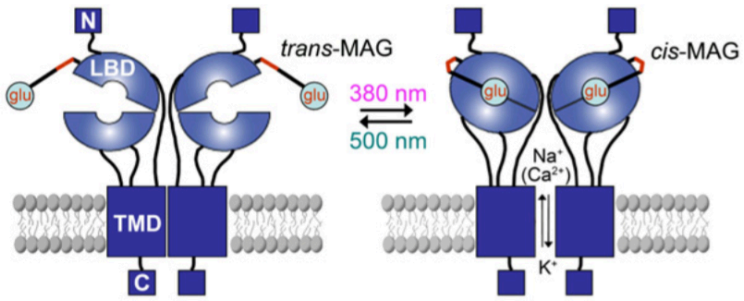

Fig. 17, Schematic representation of the light-induced activation of LiGluR. Wavelength-dependent photoisomerization of the tethered ligand, maleimide-azobenzene-glutamate (MAG) results in the activation of LiGluR, while illumination by light of 500nm leads to its inactivation (Szobota et al., 2007).

Multi-component tools include cascades of engineered proteins along with exogenous synthetic molecules, which need to be introduced into the tissue. Moreover, their presence alters the native physiological state more than the presence of a single-component tool would, and therefore, may present greater danger in terms of cell damage (Deisseroth, 2011).

6.2 Single-component tools

Single-component tools combine light-detection and effector domains into one protein, therefore reducing the size of foreign DNA or material, which needs to be introduced into the targeted neurons. They also represent the optimal measure of neuronal manipulation as was once projected by Francis Crick, by being capable of changing the properties of single neurons while not affecting other cells.

6.2.1 Microbial opsins

The capacity to detect and react to light is shared by all three domains of life. In all these domains, light-detection is often mediated by opsins; a family of seven transmembrane proteins divisible into two relatively unrelated superfamilies (Fenno et al., 2011). Type I opsins include light-driven proton pumps and channels, and are exclusively used by prokaryotes, algae and fungi (Spudich, 2006). Type II opsins encode light-sensitive G-protein coupled receptors (GPCRs), and are solely used by higher eukaryotes. Both types of opsins require a small, vitamin A-related organic cofactor, retinal, which grants the cofactor-apoprotein complex (rhodopsin) its light-sensitivity (Fenno et al., 2011). In the case of type II opsins, the absorption of a photon leads to the photoisomerization of retinal from *cis*- to *trans*-state, coupled with its dissociation from the complex (Hofmann et al., 2009). On the other hand, type I opsins, are activated by *trans* to *cis* photoisozomeration of retinal with the cofactor remaining covalently bound to the channel. Subsequent spontaneous thermal reisomerization from *cis* to *trans* completes the cyclic reaction termed “photocycle” (Haupts et al., 1997). Unfortunately, the application of microbial opsins as a possible optogenetical tool was long overlooked since the discovery of the light-driven proton pump bacteriorhodopsin (Oesterhe and Stoecken, 1973) due to general disbelief in their single-component functionality (Deisseroth, 2011).

6.2.1.1 Neural excitation

The discovery of two type I rhodopsins found in a green alga (*Chlamydomonas reinhardtii*), the light-driven proton channel Channelrhodopsin 1 (ChR1) (Nagel et al., 2002) and the light-driven cation channel Channelrhodopsin 2 (ChR2) (Nagel et al., 2003), finally led to the first application of rhodopsins as tools for neuroscience (Boyden et al., 2005). If illuminated by light of 470nm wavelength, the all-*trans* retinal undergoes isomerization, which triggers conformational changes leading to the opening of the ChR2 channel pore and subsequent membrane depolarization (Fig. 18a) (Zhang et al., 2006). The expression of ChR2 in mammalian neurons was deemed stable and safe while conserving natural basal electrical properties of the membrane (Boyden et al., 2005). Moreover, ChR2 is not only capable of generating precisely controlled spike activity while mimicking native neuronal firing (provided by diverse light

sources) (Fig. 18b), but it is also capable of producing physiologically significant subthreshold depolarizations, although in a less precise manner (Boyden et al., 2005).

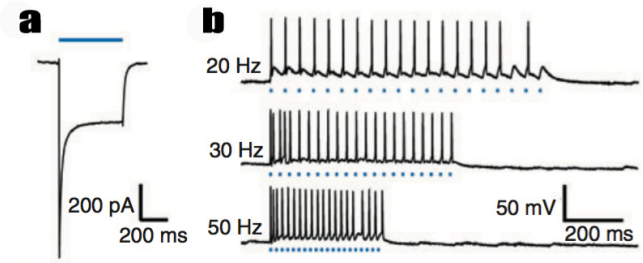

Fig. 18, *a*: An inward current evoked by a 500ms pulse of blue light in a voltage-clamped ChR2-expessing neuron. *b*: Electrical recording of a ChR2-expressing current-clamped neuron illuminated by trains (20, 30 and 50 Hz) of 10ms pulses of blue light (Zhang et al., 2006).

Although type I opsins require retinal for functioning, their *in vivo* application in mammalian central nervous system (CNS) does not require supplementary delivery of exogenous cofactors since sufficient level of native retinoids is already present in the tissue (Zhang et al., 2006). However, in the case of invertebrate models, such as *D. melanogaster* or *C. elegans*, the insufficient level of endogenous cofactor needs to be supplemented in diet (Nagel et al., 2005). Therefore, type I opsins serve as an effective single-component optogenetic tool, where one protein complex (such as the 315 amino-acid long ChR2 (Zhang et al., 2006)) detects light and also mediates the electrical response (Fig. 19). Since type I opsins are of microbial origin, one of the challenges was to ensure mammalian codon-optimization and successful membrane-trafficking in mammal neurons (Gradinaru et al., 2010). Further refinement through rational engineering of ChR2 led to versions such as ChETA with faster deactivation kinetics, capable of production of high frequency spiking with increased reliability while reducing the occurrence of extra spikes and plateau potentials (Gunaydin et al., 2010).

Furthermore, molecular engineering targeted at the ChR2 photocycle steps have rendered bi-stable mutants termed step-function opsins (SFOs). The SFOs include multiple bi-stable variants with slightly different properties, all of which lack the native time constant of ChR2 (~10ms) (Berndt et al., 2009). Most importantly, along with being activated (activation can last for minutes) by short pulses of blue light, these rhodopsins are turned off by pulses of green light, therefore allowing photoswitching similar to that of LiGluR, but with all the advantages of a single-component tool (Berndt et al., 2009).

The search for similar rhodopsins in other organisms has rendered a light-gated cation channelrhodopsin from an spheroidal alga (*Volvox carteri*), which was, due to its homology to ChR1, termed VChR1 (Zhang et al., 2008). The importance of VChR1 lies within its photostimulation wavelength, which is red-shifted compared to ChR2. This allows simultaneous control of two genetically targeted neuronal populations, since exclusive excitation of either ChR2- or VChR1-expressing neurons can be reached by using light of 406nm or 589 nm respectively (Zhang et al., 2008). Unfortunately, due to strong scatter, it is impossible to effectively separate both excitation wavelengths *in vivo*.

6.2.1.2 Neural inhibition

Light-driven neural excitation first mediated by ChR2 inspired the need for complementary light-driven neural inhibition. The search for such tool has first led to archeal light-driven chloride pumps, halorhodopsins. Among these, NpHR of *Natronomonas pharaonis* was ultimately selected, codon-optimized for mammals and tested in cultured current-clamped neurons proving its capability to mediate light-driven hyperpolarization (Zhang et al., 2007). If combined with a calcium indicator and 2PLSM, the NpHR/ChR2 system provides an all-optical tool for control and imaging of neural network (Zhang et al., 2007).

However, sub-optimal performance of NpHR, including trouble with membrane trafficking in non-mammalian models such as *C elegans.* (Husson et al., 2012), has motivated the search for alternative hyperpolarizing optogenetic tools found in light-driven proton pumps Arch and Mac (Chow et al., 2010). Their *in vivo* application in "circuit breaking" of nematode nociception and mechanosensation proved their ability to overcome certain limitations of NpHR (Husson et al., 2012) along with presenting the possibility of simultaneous silencing of multiple neuronal populations due to different excitation spectra (Chow et al., 2010). Nevertheless, neuronal silencing matching the performance of ChR2 was not achieved until the recent discovery of light-driven chloride channels from the cryptophyte *Guillardia theta* (Govorunova et al., 2015). The Anion Channel Rhodopsins (ACRs) show faster kinetics and significantly higher photosensitivity than any other tool for neural inhibition, including the third generation of Arch (Govorunova et al., 2015).

The most red-shifted among the light-driven neural silencers is the recently engineered chloride channel Jaws, a cruxhalorhodopsin capable of neural inhibition properties inferior only to ACRs (Chuong et al., 2014). It shows potential for combination with ChR2 in a system, which would offer bidirectional *in vivo* control of neural activity.

6.2.2 Biochemical optogenetics

Neural activity can be modulated by factors other than membrane voltage, such as intracellular signaling. To test the causal impact of signaling pathways, optogenetic tools obtained by replacing intracellular loops of bovine rhodopsin (a type II opsin) with those of adrenergic receptors were engineered (OptoXRs) (Airan et al., 2009). Analyses of acute brain slices revealed that the chimeric receptors were capable of light-induced production of cyclic AMP (cAMP), or inositol-3-phosphate (IP_3) and diacylglycerol (DAG) (Fig. 19). Subsequent *in vivo* experiments using transgenic animals with optoXR expression limited to nucleus accumbens, revealed that light-driven modulation of biochemical signaling in behavior-related neurons leads to behavioral changes (Airan et al., 2009).

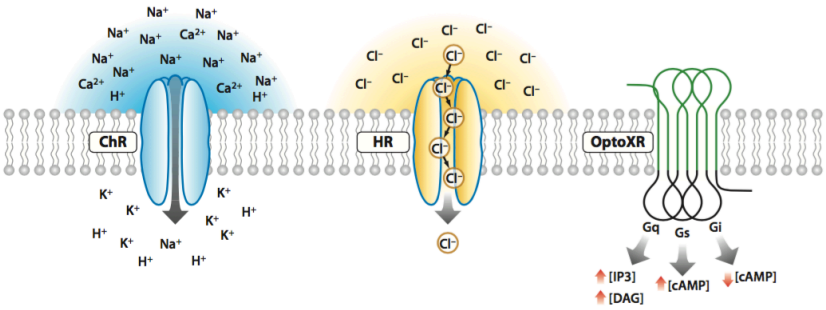

Fig. 19, General representation of the mode of function in three selected optogenetic tools. *Right:* blue-light-driven depolarizing cation channel ChR2. *Middle:* Yellow-light-driven chloride channel NpHR, capable of causing hyperpolarization. *Right:* light-activated GPCR: OptoXR capable of modulating intracellular physiology through second messengers upon illumination by green light (Fenno et al., 2011)

6.3 Light delivery

In the case of *in vivo* experiments, most notably using freely moving animals, the activation of light-driven channels proved challenging. Cortical neurons within the depth limit of 2PLSM may be photostimulated through a cranial window (Aravanis et al., 2007), while simultaneously imaged for neural activity by indicators such as VSDs (Zhang et al., 2010) or GECIs. Photostimulation of deeper structures is often performed through precise optical fiber-based laser illumination such as in the optical neural interface (ONI) (Aravanis et al., 2007). Alternatively, excitation light can be delivered by a wireless head-mountable LED device, implanted above a thinned region of the skull (Iwai et al., 2011), or implanted deep in the brain (Rossi et al., 2015) thus allowing remote control over various brain regions in a freely moving rodent.

7 Recent applications of optophysiological methods

Optogenetics and optophysiology provide the tools capable of unprecedented control and imaging of neural tissue. The following paragraphs list several recent studies illustrating the potential of these tools.

GECI-based calcium imaging (GCaMP5) was involved in studying changes of neural activity during sleep and wake of fruit flies (Bushey et al., 2015). It was shown that *Drosophila* sleep (period > 5min of immobility) is coupled with reduced spontaneous and evoked activity of Kenyon cells present in its mushroom bodies. Moreover, it was shown that sleep deprivation caused inconsistent responses of the studied neurons. The discovered sleep- or wake- related changes in neural activity of insects strongly resemble those previously observed in mammals, thus suggesting a possible link between the physiology of sleep between these two groups (Bushey et al., 2015).

Optogenetic stimulation of specific substantia nigra pars retucilaris (SNR) neurons projecting into the superior colliculus (SC) was performed on living mice to assess the role of the nigrotectal pathway in voluntary drinking behavior. It was found that the activity of SNR and SC neurons reflects the licking pattern in self-initiated drinking (electrophysiological recordings). To test the possible inhibitory role of GABAergic SNR neurons projecting into the tectum, these neurons were transduced with ChR2.

Subsequent laser stimulation of SNR in the event of drinking has resulted in a disruption of the natural behavior by significantly reducing the number of licks (Rossi et al., 2016).

Calcium imaging and optogenetic tools were also applied in a recent study regarding the role of dorsal raphe nucleus (DRN) neurons in reward signals (Li et al., 2016). GCaMP6m-based calcium imaging of serotonergic (5-HT (5-hydroxytryptamine)) DRN neurons of freely moving mice was done by fiber photometry; a method based on an optical fiber attached to a microscope setup through an optical commutator, capable of imaging the general activity of indicator-expressing cells. In this study, it was shown that 5-HT neurons are activated by natural rewards such as food, sex and social interaction. Moreover, the anticipation of a reward is accompanied by tonic activity of these neurons, which changes to phasic firing upon reaching the anticipated reward. Therefore, the data suggests that DRN neurons may perform dual roles of both anticipating and evaluating rewards. On the other hand, the GABA (*gamma*-Aminobutyric acid) -ergic neurons of DRN were found to be activated by painful stimulation (foot shock in this case) and silenced by reward, thus proposing that GABA and 5-HT neurons of DRN may be responsible for overall organization of responses to rewards and aversive stimuli. In this case, ChR2 was used for optical tagging of specific neuronal types (5-HT or GABA neurons of DRN). Optical tagging includes a device called optetrode, which is capable of verifying the cell type of a neuron by evoking ChR2-mediated APs through light stimulation and simultaneous electrical recording of responding cells (Li et al., 2016).

Finally, the application of two-photon optogenetics combined with calcium imaging in studying cortical circuits has been recently demonstrated in the article concerning disinhibition of pyramidal cells (PCs) in mice (Karnani et al., 2016). Lateral inhibition in rodent neocortex was shown to be mediated by somatostatin-expressing interneurons (SOMs) by experimentally inhibiting their activity with Arch. SOMs combined with parvalbumin-expressing (PV) interneurons and chandelier cells create a “blanket of inhibition” over the axonal arbors of PCs. Activation of these blocked PCs can be achieved through their selective disinhibition. Selective photoactivation of vasoactive intestinal peptide-expressing (VIP) interneurons through ChETA led to the conclusion that VIPs are capable of inhibiting SOMs, thus causing the disinhibition of PCs. Furthermore, the consequences of *in vivo* optogenetically-driven activation of VIPs, were directly imaged by GCaMP6s. The acquired spatiotemporal data led to the discovery that single VIP cells can form holes (60-120 μm) in the densely inhibited network. The authors suggest that this principle might be employed in the production of specific cortical circuits out of neural networks, while the holes might represent single “spotlights of attention” (Karnani et al., 2016).

8 Conclusions

The advent of molecular biology and genetics has had a significant impact on virtually every field of biology including neuroscience. Novel tools such as transgenic animal models, genetically encoded indicators of neural activity or optogenetics, along with modern methods of optical imaging are finding their way into the area classically occupied by electrophysiology. For example, two-photon calcium

imaging is capable of *in vivo* large-scale single-cell neural activity recording of specific cell-types in behaving, freely-moving animals; far beyond the achievable scale and spatial resolution of electrophysiology. However, compared to electrical recordings, which directly detect voltage-based neural activity, optical recordings use foreign molecules to translate, the otherwise invisible information, into optically detectable fluorescence. Consequently, optophysiological methods import a number of additional variables into the process of detection, thus negatively affecting the achievable precision. In summary, due to the underlying mechanisms of signal generation and detection, neural activity reporting based on fluorescent probes cannot reach the precision of classical electrical recording and requires its support if to be trusted completely. The role of novel, genetically targetable optical methods reviewed in this text is not to replace classical, well-attained methods of neuroscience, but to serve as their complementary partner suitable for genetically targeted large-scale recordings (or manipulations), with precision limited to physiologically significant changes. Combined in innovative experimental protocols, these approaches will hopefully provide the data required for the understanding of the fundamental principles underlying the function of neural tissue.

Further refinement of the existing genetically encoded tools for optical recording and control (mainly through structure-guided rational mutagenesis) will hopefully lead to proteins with better kinetics and overall performance. The ultimate goal is to reach the resolution, which would allow non-invasive recording of physiologically significant events with detection reliability matching supporting electrophysiological data.

9 References

Abbe E (1873) Beiträge zur Theorie des Mikroskops und der mikroskopischen Wahrnehmung. Archiv für mikroskopische Anatomie 9:413-418.

Ahmed BY, Chakravarthy S, Eggers R, Hermens W, Zhang JY, Niclou SP, Levelt C, Sablitzky F, Anderson PN, Lieberman AR, Verhaagen J (2004) Efficient delivery of Cre-recombinase to neurons in vivo and stable transduction of neurons using adeno-associated and lentiviral vectors - art. no. 5. Bmc Neuroscience 5:11.

Ahrens MB, Orger MB, Robson DN, Li JM, Keller PJ (2013) Whole-brain functional imaging at cellular resolution using light-sheet microscopy. Nature Methods 10:413-420.

Airan RD, Thompson KR, Fenno LE, Bernstein H, Deisseroth K (2009) Temporally precise in vivo control of intracellular signalling. Nature 458:1025-1029.

Akerboom J, Rivera JDV, Guilbe MMR, Malave ECA, Hernandez HH, Tian L, Hires SA, Marvin JS, Looger LL, Schreiter ER (2009) Crystal Structures of the GCaMP Calcium Sensor Reveal the Mechanism of Fluorescence Signal Change and Aid Rational Design. Journal of Biological Chemistry 284:6455-6464.

Akerboom J et al. (2012) Optimization of a GCaMP Calcium Indicator for Neural Activity Imaging. Journal of Neuroscience 32:13819-13840.

Aravanis AM, Wang LP, Zhang F, Meltzer LA, Mogri MZ, Schneider MB, Deisseroth K (2007) An optical neural interface: in vivo control of rodent motor cortex with integrated fiberoptic and optogenetic technology. Journal of Neural Engineering 4:S143-S156.

Ataka K, Pieribone VA (2002) A genetically targetable fluorescent probe of channel gating with rapid kinetics. Biophysical Journal 82:509-516.

Baird GS, Zacharias DA, Tsien RY (1999) Circular permutation and receptor insertion within green fluorescent proteins. Proceedings of the National Academy of Sciences of the United States of America 96:11241-11246.

Baker BJ, Kosmidis EK, Vucinic D, Falk CX, Cohen LB, Djurisic M, Zecevic D (2005) Imaging brain activity with voltage- and calcium-sensitive dyes. Cellular and Molecular Neurobiology 25:245-282.

Baker BJ, Mutoh H, Dimitrov D, Akemann W, Perron A, Iwamoto Y, Jin L, Cohen LB, Isacoff EY, Pieribone VA, Hughes T, Knopfel T (2008) Genetically encoded fluorescent sensors of membrane potential. Brain Cell Biology 36:53-67.

Baker PF, Hodgkin AL, Ridgway EB (1971) Depolarization and calcium entry in squid giant axons. Journal of Physiology-London 218:709-755.

Bellen HJ, Tong C, Tsuda H (2010) 100 years of Drosophila research and its impact on vertebrate neuroscience: a history lesson for the future. Nature Reviews Neuroscience 11:514-522.
Berger T, Borgdorff A, Crochet S, Neubauer FB, Lefort S, Fauvet B, Ferezou I, Carleton A, Luscher HR, Petersen CCH (2007) Combined voltage and calcium epifluorescence Imaging in vitro and in vivo reveals subthreshold and suprathreshold dynamics of mouse barrel cortex. Journal of Neurophysiology 97:3751-3762.
Berndt A, Yizhar O, Gunaydin LA, Hegemann P, Deisseroth K (2009) Bi-stable neural state switches. Nature Neuroscience 12:229-234.
Berning S, Willig KI, Steffens H, Dibaj P, Hell SW (2012) Nanoscopy in a Living Mouse Brain. Science 335:551-551.
Berridge MJ (1998) Neuronal calcium signaling. Neuron 21:13-26.
Bockamp E, Maringer M, Spangenberg C, Fees S, Fraser S, Eshkind L, Oesch F, Zabel B (2002) Of mice and models: improved animal models for biomedical research. Physiological Genomics 11:115-132.
Boyden ES, Zhang F, Bamberg E, Nagel G, Deisseroth K (2005) Millisecond-timescale, genetically targeted optical control of neural activity. Nature Neuroscience 8:1263-1268.
Breunig JJ, Silbereis J, Vaccarino FM, Sestan N, Rakic P (2007) Notch regulates cell fate and dendrite morphology of newborn neurons in the postnatal dentate gyrus. Proceedings of the National Academy of Sciences of the United States of America 104:20558-20563.
Buning H, Perabo L, Coutelle O, Quadt-Humme S, Hallek M (2008) Recent developments in adeno-associated virus vector technology. Journal of Gene Medicine 10:717-733.
Bushey D, Tononi G, Cirelli C (2015) Sleep- and wake-dependent changes in neuronal activity and reactivity demonstrated in fly neurons using in vivo calcium imaging. Proceedings of the National Academy of Sciences of the United States of America 112:4785-4790.
Buzsaki G (2004) Large-scale recording of neuronal ensembles. Nature Neuroscience 7:446-451.
Callaway EM, Katz LC (1993) Photostimulation using caged glutamate reveals functional circuitry in living brain-slices. Proceedings of the National Academy of Sciences of the United States of America 90:7661-7665.
Cao G, Platisa J, Pieribone VA, Raccuglia D, Kunst M, Nitabach MN (2013) Genetically Targeted Optical Electrophysiology in Intact Neural Circuits. Cell 154:904-913.
Capecchi MR (1989) Altering the genome by homologous recombination. Science 244:1288-1292.
Chen TW, Wardill TJ, Sun Y, Pulver SR, Renninger SL, Baohan A, Schreiter ER, Kerr RA, Orger MB, Jayaraman V, Looger LL, Svoboda K, Kim DS (2013) Ultrasensitive fluorescent proteins for imaging neuronal activity. Nature 499:295-+.
Chereau R, Tonnesen J, Nagerl UV (2015) STED microscopy for nanoscale imaging in living brain slices. Methods 88:57-66.
Chorev E, Epsztein J, Houweling AR, Lee AK, Brecht M (2009) Electrophysiological recordings from behaving animals-going beyond spikes. Current Opinion in Neurobiology 19:513-519.
Chow BY, Han X, Dobry AS, Qian XF, Chuong AS, Li MJ, Henninger MA, Belfort GM, Lin YX, Monahan PE, Boyden ES (2010) High-performance genetically targetable optical neural silencing by light-driven proton pumps. Nature 463:98-102.
Chuong AS et al. (2014) Noninvasive optical inhibition with a red-shifted microbial rhodopsin. Nature Neuroscience 17:1123-1129.
Cohen LB, Salzberg BM, Grinvald A (1978) Optical methods for monitoring neuron activity. Annual Review of Neuroscience 1:171-182.
Combs C (2010) Fluorescence Microscopy: A Concise Guide to Current Imaging Methods. In: *Current Protocols in Neuroscience*.
Crick F (1999) The impact of molecular biology on neuroscience. Philosophical Transactions of the Royal Society of London Series B-Biological Sciences 354:2021-2025.
Crick FHC (1979) Thinking about the brain. Scientific American 241:219-&.
Crochet S, Petersen CCH (2006) Correlating whisker behavior with membrane potential in barrel cortex of awake mice. Nature Neuroscience 9:608-610.
Deisseroth K (2011) Optogenetics. Nature Methods 8:26-29.
Denk W, Strickler JH, Webb WW (1990) 2-photon laser scanning fluorescence microscopy. Science 248:73-76.
Dimitrov D, He Y, Mutoh H, Baker BJ, Cohen L, Akemann W, Knopfel T (2007) Engineering and Characterization of an Enhanced Fluorescent Protein Voltage Sensor. Plos One 2:5.
Dombeck DA, Khabbaz AN, Collman F, Adelman TL, Tank DW (2007) Imaging large-scale neural activity with cellular resolution in awake, mobile mice. Neuron 56:43-57.
Driever W, SolnicaKrezel L, Schier AF, Neuhauss SCF, Malicki J, Stemple DL, Stainier DYR, Zwartkruis F, Abdelilah S, Rangini Z, Belak J, Boggs C (1996) A genetic screen for mutations affecting embryogenesis in zebrafish. Development 123:37-46.
Drobizhev M, Makarov NS, Tillo SE, Hughes TE, Rebane A (2011) Two-photon absorption properties of fluorescent proteins. Nature Methods 8:393-399.
Dunn AK, Wallace VP, Coleno M, Berns MW, Tromberg BJ (2000) Influence of optical properties on two-photon fluorescence imaging in turbid samples. Applied Optics 39:1194-1201.
Dunn KW, Mayor S, Myers JN, Maxfield FR (1994) Applications of ratio fluorescence microscopy in the study of cell physiology. Faseb Journal 8:573-582.
Erni R, Rossell MD, Kisielowski C, Dahmen U (2009) Atomic-Resolution Imaging with a Sub-50-pm Electron Probe. Physical Review Letters 102:4.
Feil R, Wagner J, Metzger D, Chambon P (1997) Regulation of Cre recombinase activity by mutated estrogen receptor ligand-binding domains. Biochemical and Biophysical Research Communications 237:752-757.
Fenno L, Yizhar O, Deisseroth K (2011) The Development and Application of Optogenetics. In: Annual Review of Neuroscience, Vol 34 (Hyman SE, Jessell TM, Shatz CJ, Stevens CF, Zoghbi HY, eds), pp 389-412. Palo Alto: Annual Reviews.
Ferezou I, Haiss F, Gentet LJ, Aronoff R, Weber B, Petersen CCH (2007) Spatiotemporal dynamics of cortical sensorimotor integration in behaving mice. Neuron 56:907-923.

Friedrich RW, Korsching SI (1997) Combinatorial and chemotopic odorant coding in the zebrafish olfactory bulb visualized by optical imaging. Neuron 18:737-752.
Gong YY, Wagner MJ, Li JZ, Schnitzer MJ (2014) Imaging neural spiking in brain tissue using FRET-opsin protein voltage sensors. Nature Communications 5:11.
Gordon JW, Scangos GA, Plotkin DJ, Barbosa JA, Ruddle FH (1980) Genetic transformation of mouse embryos by microinjection of purified DNA. Proceedings of the National Academy of Sciences of the United States of America-Biological Sciences 77:7380-7384.
Gossen M, Bujard H (1992) Tight control of gene expression in mammalian cells by tetracycline-responsive promoters. Proceedings of the National Academy of Sciences of the United States of America 89:5547-5551.
Gossen M, Freundlieb S, Bender G, Muller G, Hillen W, Bujard H (1995) Transcriptional activation by tetracyclines in mammalian cells. Science 268:1766-1769.
Govorunova EG, Sineshchekov OA, Janz R, Liu XQ, Spudich JL (2015) Natural light-gated anion channels: A family of microbial rhodopsins for advanced optogenetics. Science 349:647-650.
Grabarek Z (2006) Structural basis for diversity of the EF-hand calcium-binding proteins. Journal of Molecular Biology 359:509-525.
Gradinaru V, Zhang F, Ramakrishnan C, Mattis J, Prakash R, Diester I, Goshen I, Thompson KR, Deisseroth K (2010) Molecular and Cellular Approaches for Diversifying and Extending Optogenetics. Cell 141:154-165.
Grewe BF, Langer D, Kasper H, Kampa BM, Helmchen F (2010) High-speed in vivo calcium imaging reveals neuronal network activity with near-millisecond precision. Nature Methods 7:399-U391.
Griffith JD, Comeau L, Rosenfield S, Stansel RM, Bianchi A, Moss H, de Lange T (1999) Mammalian telomeres end in a large duplex loop. Cell 97:503-514.
Grutzendler J, Kasthuri N, Gan WB (2002) Long-term dendritic spine stability in the adult cortex. Nature 420:812-816.
Grynkiewicz G, Poenie M, Tsien RY (1985) A new generation of Ca2+ indicators with greatly improved fluorescence properties. Journal of Biological Chemistry 260:3440-3450.
Gunaydin LA, Yizhar O, Berndt A, Sohal VS, Deisseroth K, Hegemann P (2010) Ultrafast optogenetic control. Nature Neuroscience 13:387-U327.
Guo S (2004) Linking genes to brain, behavior and neurological diseases: what can we learn from zebrafish? Genes Brain and Behavior 3:63-74.
Gustafsson MGL (2000) Surpassing the lateral resolution limit by a factor of two using structured illumination microscopy. Journal of Microscopy-Oxford 198:82-87.
Göppert-Mayer M (1931) Über Elementarakte mit zwei Quantensprüngen. Annalen der Physik 401:273-294.
Haupts U, Tittor J, Bamberg E, Oesterhelt D (1997) General concept fur ion translocation by halobacterial retinal proteins: The isomerization/switch/transfer (IST) model. Biochemistry 36:2-7.
Hayashi S, McMahon AP (2002) Efficient recombination in diverse tissues by a tamoxifen-inducible form of Cre: A tool for temporally regulated gene activation/inactivation in the mouse. Developmental Biology 244:305-318.
Heim N, Griesbeck O (2004) Genetically encoded indicators of cellular calcium dynamics based on troponin C and green fluorescent protein. Journal of Biological Chemistry 279:14280-14286.
Heim R, Cubitt AB, Tsien RY (1995) Improved green fluorescence. Nature 373:663-664.
Hell SW, Wichmann J (1994) Breaking the diffraction resolution limit by stimulated emission: stimulated-emission-depletion fluorescence microscopy. Optics Letters 19:780-782.
Helmchen F, Denk W (2005) Deep tissue two-photon microscopy. Nature Methods 2:932-940.
Hendel T, Mank M, Schnell B, Griesbeck O, Borst A, Reiff DF (2008) Fluorescence changes of genetic calcium indicators and OGB-1 correlated with neural activity and calcium in vivo and in vitro. Journal of Neuroscience 28:7399-7411.
Hodgkin AL, Huxley AF (1952) A quantitative description of membrane current and its application to conduction and excitation in nerve. Journal of Physiology-London 117:500-544.
Hofmann KP, Scheerer P, Hildebrand PW, Choe HW, Park JH, Heck M, Ernst OP (2009) A G protein-coupled receptor at work: the rhodopsin model. Trends in Biochemical Sciences 34:540-552.
Horikawa K, Yamada Y, Matsuda T, Kobayashi K, Hashimoto M, Matsu-ura T, Miyawaki A, Michikawa T, Mikoshiba K, Nagai T (2010) Spontaneous network activity visualized by ultrasensitive Ca2+ indicators, yellow Cameleon-Nano. Nature Methods 7:729-U788.
Horton NG, Wang K, Kobat D, Clark CG, Wise FW, Schaffer CB, Xu C (2013) In vivo three-photon microscopy of subcortical structures within an intact mouse brain. Nature Photonics 7:205-209.
Huang Z (2010) Genetic labeling of neurons in mouse brain. In, p 199. Cold Spring Harbor, New York: A Laboratory Manual Cold Spring Harbor Laboratory Press.
Hubel DH, Wiesel TN (1959) Receptive fields of single neurones in the cat's striate cortex. Journal of Physiology-London 148:574-591.
Hulikova A, Vaughan-Jones RD, Swietach P (2011) Dual Role of CO2/HCO3- Buffer in the Regulation of Intracellular pH of Three-dimensional Tumor Growths. Journal of Biological Chemistry 286:13815-13826.
Husson SJ, Liewald JF, Schultheis C, Stirman JN, Lu H, Gottschalk A (2012) Microbial Light-Activatable Proton Pumps as Neuronal Inhibitors to Functionally Dissect Neuronal Networks in C. elegans. Plos One 7:14.
Ikura M, Clore GM, Gronenborn AM, Zhu G, Klee CB, Bax A (1992) Solution structure of a calmodulin-target peptide complex by multidimensional NMR. Science 256:632-638.
IOM IoM, NRC NRC (2012) Animals in Neuroscience Research. In: International Animal Research Regulations: Impact on Neuroscience Research: Workshop Summary. Washington, DC: The National Academies Press.
Issa JB, Haeffele BD, Agarwal A, Bergles DE, Young ED, Yue DT (2014) Multiscale Optical Ca2+ Imaging of Tonal Organization in Mouse Auditory Cortex. Neuron 83:944-959.

Iwai Y, Honda S, Ozeki H, Hashimoto M, Hirase H (2011) A simple head-mountable LED device for chronic stimulation of optogenetic molecules in freely moving mice. Neuroscience Research 70:124-127.
Jacobs RE, Cherry SR (2001) Complementary emerging techniques: high-resolution PET and MRI. Current Opinion in Neurobiology 11:621-629.
Jay DG (1988) Selective destruction of protein function by chromophore-assisted laser inactivation. Proceedings of the National Academy of Sciences of the United States of America 85:5454-5458.
Jung JC, Schnitzer MJ (2003) Multiphoton endoscopy. Optics Letters 28:902-904.
Jung JC, Mehta AD, Aksay E, Stepnoski R, Schnitzer MJ (2004) In vivo mammalian brain Imaging using one- and two-photon fluorescence microendoscopy. Journal of Neurophysiology 92:3121-3133.
Kabanova A, Pabst M, Lorkowski M, Braganza O, Boehlen A, Nikbakht N, Pothmann L, Vaswani AR, Musgrove R, Di Monte DA, Sauvage M, Beck H, Blaess S (2015) Function and developmental origin of a mesocortical inhibitory circuit. Nature Neuroscience 18:872-U314.
Kapuscinski J (1995) DAPI: a DNA-specific fluorescent probe. Biotechnic & Histochemistry 70:220-233.
Karnani MM, Jackson J, Ayzenshtat I, Sichani AH, Manoocheri K, Kim S, Yuste R (2016) Opening Holes in the Blanket of Inhibition: Localized Lateral Disinhibition by VIP Interneurons. Journal of Neuroscience 36:3471-3480.
Karra D, Dahm R (2010) Transfection Techniques for Neuronal Cells. Journal of Neuroscience 30:6171-6177.
Keller PJ, Schmidt AD, Wittbrodt J, Stelzer EHK (2008) Reconstruction of Zebrafish Early Embryonic Development by Scanned Light Sheet Microscopy. Science 322:1065-1069.
Kepecs A, Uchida N, Zariwala HA, Mainen ZF (2008) Neural correlates, computation and behavioural impact of decision confidence. Nature 455:227-U255.
Kerr JND, Greenberg D, Helmchen F (2005) Imaging input and output of neocortical networks in vivo. Proceedings of the National Academy of Sciences of the United States of America 102:14063-14068.
Kimmel CB (1993) Patterning the brain of the zebrafish embryo. Annual Review of Neuroscience 16:707-732.
Kita EM, Scott EK, Goodhill GJ (2015) Topographic wiring of the retinotectal connection in zebrafish. Developmental Neurobiology 75:542-556.
Knopfel T, Diez-Garcia J, Akemann W (2006) Optical probing of neuronal circuit dynamics: genetically encoded versus classical fluorescent sensors. Trends in Neurosciences 29:160-166.
Knopfel T, Tomita K, Shimazaki R, Sakai R (2003) Optical recordings of membrane potential using genetically targeted voltage-sensitive fluorescent proteins. Methods 30:42-48.
Kobat D, Horton NG, Xu C (2011) In vivo two-photon microscopy to 1.6-mm depth in mouse cortex. Journal of Biomedical Optics 16:4.
Kretsinger RH, Nockolds CE (1973) Carp muscle calcium-binding protein. II. Structure determination and general description. Journal of Biological Chemistry 248:3313-3326.
Kuhlman SJ, Huang ZJ (2008) High-Resolution Labeling and Functional Manipulation of Specific Neuron Types in Mouse Brain by Cre-Activated Viral Gene Expression. Plos One 3:11.
Lakso M, Sauer B, Mosinger B, Lee EJ, Manning RW, Yu SH, Mulder KL, Westphal H (1992) Targeted oncogene activation by site-specific recombination in transgenic mice. Proceedings of the National Academy of Sciences of the United States of America 89:6232-6236.
Lambert R (2007) Breeding Strategies for Maintaining Colonies of Laboratory Mice. In: (Laboratory TJ, ed).
Levene MJ, Dombeck DA, Kasischke KA, Molloy RP, Webb WW (2004) In vivo multiphoton microscopy of deep brain tissue. Journal of Neurophysiology 91:1908-1912.
Li Y, Zhong WX, Wang DQ, Feng QR, Liu ZX, Zhou JF, Jia CY, Hu F, Zeng JW, Guo QC, Fu L, Luo MM (2016) Serotonin neurons in the dorsal raphe nucleus encode reward signals. Nature Communications 7:15.
Lima SQ, Miesenbock G (2005) Remote control of behavior through genetically targeted photostimulation of neurons. Cell 121:141-152.
Lippert MT, Takagaki K, Xu WF, Huang XY, Wu JY (2007) Methods for voltage-sensitive dye imaging of rat cortical activity with high signal-to-noise ratio. Journal of Neurophysiology 98:502-512.
Llano I, Dipolo R, Marty A (1994) Calcium-induced calcium release in cerebellar Purkinje cells. Neuron 12:663-673.
Lutcke H, Helmchen F (2011) Two-photon imaging and analysis of neural network dynamics. Reports on Progress in Physics 74:19.
Magee JC, Johnston D (1995) Characterization of single voltage-gated Na+ and Ca2+ channels in apical dendrites of rat CA1 pyramidal neurons. Journal of Physiology-London 487:67-90.
Mainen ZF, Maletic-Savatic M, Shi SH, Hayashi Y, Malinow R, Svoboda K (1999) Two-photon imaging in living brain slices. Methods-a Companion to Methods in Enzymology 18:231-+.
Mank M, Griesbeck O (2008) Genetically encoded calcium indicators. Chemical Reviews 108:1550-1564.
Mank M, Reiff DF, Heim N, Friedrich MW, Borst A, Griesbeck O (2006) A FRET-based calcium biosensor with fast signal kinetics and high fluorescence change. Biophysical Journal 90:1790-1796.
Mank M, Santos AF, Direnberger S, Mrsic-Flogel TD, Hofer SB, Stein V, Hendel T, Reiff DF, Levelt C, Borst A, Bonhoeffer T, Hubener M, Griesbeck O (2008) A genetically encoded calcium indicator for chronic in vivo two-photon imaging. Nature Methods 5:805-811.
Mantini D, Corbetta M, Romani GL, Orban GA, Vanduffel W (2013) Evolutionarily Novel Functional Networks in the Human Brain? Journal of Neuroscience 33:3259-3275.
Margrie TW, Meyer AH, Caputi A, Monyer H, Hasan MT, Schaefer AT, Denk W, Brecht M (2003) Targeted whole-cell recordings in the mammalian brain in vivo. Neuron 39:911-918.
Mayer G, Heckel A (2006) Biologically active molecules with a "light switch". Angewandte Chemie-International Edition 45:4900-4921.

McHenry JZ, Leon A, Matthaei KI, Cohen DR (1998) Overexpression of fra-2 in transgenic mice perturbs normal eye development. Oncogene 17:1131-1140.
Miklosi A, Andrew RJ (1999) Right eye use associated with decision to bite in zebrafish. Behavioural Brain Research 105:199-205.
Minta A, Kao JPY, Tsien RY (1989) Fluorescent indicators for cytosolic calcium based on rhodamine and fluorescein chromophores. Journal of Biological Chemistry 264:8171-8178.
Miyawaki A, Llopis J, Heim R, McCaffery JM, Adams JA, Ikura M, Tsien RY (1997) Fluorescent indicators for Ca2+ based on green fluorescent proteins and calmodulin. Nature 388:882-887.
Moore T, Armstrong KM (2003) Selective gating of visual signals by microstimulation of frontal cortex. Nature 421:370-373.
Murata Y, Iwasaki H, Sasaki M, Inaba K, Okamura Y (2005) Phosphoinositide phosphatase activity coupled to an intrinsic voltage sensor. Nature 435:1239-1243.
Mutze J, Iyer V, Macklin JJ, Colonell J, Karsh B, Petrasek Z, Schwille P, Looger LL, Lavis LD, Harris TD (2012) Excitation Spectra and Brightness Optimization of Two-Photon Excited Probes. Biophysical Journal 102:934-944.
Nagai T, Sawano A, Park ES, Miyawaki A (2001) Circularly permuted green fluorescent proteins engineered to sense Ca2+. Proceedings of the National Academy of Sciences of the United States of America 98:3197-3202.
Nagai T, Yamada S, Tominaga T, Ichikawa M, Miyawaki A (2004) Expanded dynamic range of fluorescent indicators for Ca2+ by circularly permuted yellow fluorescent proteins. Proceedings of the National Academy of Sciences of the United States of America 101:10554-10559.
Nagel G, Brauner M, Liewald JF, Adeishvili N, Bamberg E, Gottschalk A (2005) Light activation of channelrhodopsin-2 in excitable cells of Caenorhabditis elegans triggers rapid Behavioral responses. Current Biology 15:2279-2284.
Nagel G, Ollig D, Fuhrmann M, Kateriya S, Mustl AM, Bamberg E, Hegemann P (2002) Channelrhodopsin-1: A light-gated proton channel in green algae. Science 296:2395-2398.
Nagel G, Szellas T, Huhn W, Kateriya S, Adeishvili N, Berthold P, Ollig D, Hegemann P, Bamberg E (2003) Channelrhodopsin-2, a directly light-gated cation-selective membrane channel. Proceedings of the National Academy of Sciences of the United States of America 100:13940-13945.
Nagerl UV, Willig KI, Hein B, Hell SW, Bonhoeffer T (2008) Live-cell imaging of dendritic spines by STED microscopy. Proceedings of the National Academy of Sciences of the United States of America 105:18982-18987.
Nakai J, Ohkura M, Imoto K (2001) A high signal-to-noise Ca2+ probe composed of a single green fluorescent protein. Nature Biotechnology 19:137-141.
Neumann E, Schaeferridder M, Wang Y, Hofschneider PH (1982) Gene transfer into mouse lyoma cells by electroporation in high electric fields. Embo Journal 1:841-845.
Noguchi J, Nagaoka A, Watanabe S, Ellis-Davies GCR, Kitamura K, Kano M, Matsuzaki M, Kasai H (2011) In vivo two-photon uncaging of glutamate revealing the structure-function relationships of dendritic spines in the neocortex of adult mice. Journal of Physiology-London 589:2447-2457.
Oesterhe D, Stoecken W (1973) Functions of a new photoreceptor membrane. Proceedings of the National Academy of Sciences of the United States of America 70:2853-2857.
Oheim M, Beaurepaire E, Chaigneau E, Mertz J, Charpak S (2001) Two-photon microscopy in brain tissue: parameters influencing the imaging depth. Journal of Neuroscience Methods 111:29-37.
Orban PC, Chui D, Marth JD (1992) Tissue- and site-specific DNA recombination in transgenic mice. Proceedings of the National Academy of Sciences of the United States of America 89:6861-6865.
Palmer AE, Giacomello M, Kortemme T, Hires SA, Lev-Ram V, Baker D, Tsien RY (2006) Ca2+ indicators based on computationally redesigned calmodulin-peptide pairs. Chemistry & Biology 13:521-530.
Paredes RM, Etzler JC, Watts LT, Zheng W, Lechleiter JD (2008) Chemical calcium indicators. Methods 46:143-151.
Pavlou HJ, Goodwin SF (2013) Courtship behavior in Drosophila melanogaster: towards a 'courtship connectome'. Current Opinion in Neurobiology 23:76-83.
Pelletier J, Sonenberg N (1988) Internal initiation of translation of eukaryotic mRNA directed by a sequence derived from poliovirus RNA. Nature 334:320-325.
Petersen CCH, Grinvald A, Sakmann B (2003) Spatiotemporal dynamics of sensory responses in layer 2/3 of rat barrel cortex measured in vivo by voltage-sensitive dye imaging combined with whole-cell voltage recordings and neuron reconstructions. Journal of Neuroscience 23:1298-1309.
Phan TG, Bullen A (2010) Practical intravital two-photon microscopy for immunological research: faster, brighter, deeper. Immunology and Cell Biology 88:438-444.
Poulson D (1950) Histogenesis, organogenesis and differentiation in the embryo of Drosophila melanogaster. In. New York.
Provost E, Rhee J, Leach SD (2007) Viral 2A peptides allow expression of multiple proteins from a single ORF in Transgenic zebrafish embryos. Genesis 45:625-629.
Radcliffe PA, Mitrophanous KA (2004) Multiple gene products from a single vector: 'self-cleaving' 2A peptides. Gene Therapy 11:1673-1674.
Ribrault C, Sekimoto K, Triller A (2011) From the stochasticity of molecular processes to the variability of synaptic transmission. Nature Reviews Neuroscience 12:375-387.
Riddle DL, Blumenthal T, Meyer BJ, Priess JR (1997) Section I, The Biological Model. In: C. elegans II. Cold Spring Harbor (NY): Cold Spring Harbor Laboratory Press.
Roelfsema PR, Treue S (2014) Basic Neuroscience Research with Nonhuman Primates: A Small but Indispensable Component of Biomedical Research. Neuron 82:1200-1204.
Ross WN, Salzberg BM, Cohen LB, Grinvald A, Davila HV, Waggoner AS, Wang CH (1977) Changes in absorption, fluorescence, dichroism, and birefringence in stained giant axons: optical measurement of membrane potential. Journal of Membrane Biology 33:141-183.
Rossi MA, Go V, Murphy T, Fu QH, Morizio J, Yin HH (2015) A wirelessly controlled implantable LED system for deep brain optogenetic stimulation. Frontiers in Integrative Neuroscience 9:7.

Rossi MA, Li HE, Lu D, Kim IH, Bartholomew RA, Gaidis E, Barter JW, Kim N, Cai MT, Soderling SH, Yin HH (2016) A GABAergic nigrotectal pathway for coordination of drinking behavior. Nat Neurosci 19:742-748.
Rust MJ, Bates M, Zhuang XW (2006) Sub-diffraction-limit imaging by stochastic optical reconstruction microscopy (STORM). Nature Methods 3:793-795.
Sadowski PD (1995) The FLP recombinase of the Saccharomyces cerevisiae 2 microns plasmid attaches covalently to DNA via a phosphotyrosyl linkage. Progress in Nucleic Acid Research and Molecular Biology, Vol 51 51:53-91.
Sauer B, Henderson N (1988) Site-specific DNA recombination in mammalian cells by the Cre recombinase of bacteriophage P1. Proceedings of the National Academy of Sciences of the United States of America 85:5166-5170.
Schermelleh L, Heintzmann R, Leonhardt H (2010) A guide to super-resolution fluorescence microscopy. Journal of Cell Biology 190:165-175.
Schmucker D, Su AL, Beermann A, Jackle H, Jay DG (1994) Chromophore-assisted laser inactivation of patched protein switches cell fate in the larval visual system of Drosophila. Proceedings of the National Academy of Sciences of the United States of America 91:2664-2668.
Schwartz CJE, Sadowski PD (1989) FLP Recombinase of the 2 μm circle plasmid of *Saccharomyces cerevisiae* bends its DNA target: Isolation of FLP mutants defective in DNA bending. Journal of Molecular Biology 205:647-658.
Sengupta P, Samuel ADT (2009) Caenorhabditis elegans: a model system for systems neuroscience. Current Opinion in Neurobiology 19:637-643.
Shaner NC, Steinbach PA, Tsien RY (2005) A guide to choosing fluorescent proteins. Nature Methods 2:905-909.
Shaw P (1995) Comparison of Wide-Field/Deconvolution and Confocal Microscopy for 3D Imaging. In: Handbook of Biological Confocal Microscopy (Pawley J, ed), pp 373-387: Springer US.
Shevtsova Z, Malik JMI, Michel U, Bahr M, Kugler S (2005) Promoters and serotypes: targeting of adeno-associated virus vectors for gene transfer in the rat central nervous system in vitro and in vivo. Experimental Physiology 90:53-59.
Siegel MS, Isacoff EY (1997) A genetically encoded optical probe of membrane voltage. Neuron 19:735-741.
Smedemark-Margulies N, Trapani JG (2013) Tools, methods, and applications for optophysiology in neuroscience. Frontiers in Molecular Neuroscience 6:13.
Smith AM, Mancini MC, Nie SM (2009) Bioimaging: Second window for in vivo imaging. Nature Nanotechnology 4:710-711.
Sordillo LA, Pu Y, Pratavieira S, Budansky Y, Alfano RR (2014) Deep optical imaging of tissue using the second and third near-infrared spectral windows. Journal of Biomedical Optics 19:6.
Spudich JL (2006) The multitalented microbial sensory rhodopsins. Trends in Microbiology 14:480-487.
St-Pierre F, Marshall JD, Yang Y, Gong YY, Schnitzer MJ, Lin MZ (2014) High-fidelity optical reporting of neuronal electrical activity with an ultrafast fluorescent voltage sensor. Nature Neuroscience 17:884-889.
Stables J, Mattheakis LC, Chang R, Rees S (2000) Recombinant aequorin as reporter of changes in intracellular calcium in mammalian cells. Applications of Chimeric Genes and Hybrid Proteins Pt B 327:456-471.
Sternberg N, Hamilton D (1981) Bacteriophage P1 site-specific recombination. I. Recombination between loxP sites. Journal of Molecular Biology 150:467-486.
Stewart AM, Braubach O, Spitsbergen J, Gerlai R, Kalueffl AV (2014) Zebrafish models for translational neuroscience research: from tank to bedside. Trends in Neurosciences 37:264-278.
Stosiek C, Garaschuk O, Holthoff K, Konnerth A (2003) In vivo two-photon calcium imaging of neuronal networks. Proceedings of the National Academy of Sciences of the United States of America 100:7319-7324.
Streisinger G, Walker C, Dower N, Knauber D, Singer F (1981) Production of clones of homozygous diploid zebra fish (Brachydanio rerio). Nature 291:293-296.
Szobota S, Gorostiza P, Del Bene F, Wyart C, Fortin DL, Kolstad KD, Tulyathan O, Volgraf M, Numano R, Aaron HL, Scott EK, Kramer RH, Flannery J, Baier H, Trauner D, Isacoff EY (2007) Remote control of neuronal activity with a light-gated glutamate receptor. Neuron 54:535-545.
Taniguchi H, He M, Wu P, Kim S, Paik R, Sugino K, Kvitsani D, Fu Y, Lu JT, Lin Y, Miyoshi G, Shima Y, Fishell G, Nelson SB, Huang ZJ (2011) A Resource of Cre Driver Lines for Genetic Targeting of GABAergic Neurons in Cerebral Cortex. Neuron 71:995-1013.
Tasaki I, Watanabe A, Sandlin R, Carnay L (1968) Changes in fluorescence, turbidity, and birefringence associated with nerve excitation. Proceedings of the National Academy of Sciences of the United States of America 61:883-&.
Thestrup T, Litzlbauer J, Bartholomaus I, Mues M, Russo L, Dana H, Kovalchuk Y, Liang YJ, Kalamakis G, Laukat Y, Becker S, Witte G, Geiger A, Allen T, Rome LC, Chen TW, Kim DS, Garaschuk O, Griesinger C, Griesbeck O (2014) Optimized ratiometric calcium sensors for functional in vivo imaging of neurons and T lymphocytes. Nature Methods 11:175-+.
Thomas D, Tovey SC, Collins TJ, Bootman MD, Berridge MJ, Lipp P (2000) A comparison of fluorescent Ca2+ indicator properties and their use in measuring elementary and global Ca2+ signals. Cell Calcium 28:213-223.
Thomas KR, Capecchi MR (1987) Site-directed mutagenesis by gene targeting in mouse embryo-derived stem cells. Cell 51:503-512.
Tian L, Hires SA, Mao T, Huber D, Chiappe ME, Chalasani SH, Petreanu L, Akerboom J, McKinney SA, Schreiter ER, Bargmann CI, Jayaraman V, Svoboda K, Looger LL (2009) Imaging neural activity in worms, flies and mice with improved GCaMP calcium indicators. Nature Methods 6:875-U113.
Trachtenberg JT, Chen BE, Knott GW, Feng GP, Sanes JR, Welker E, Svoboda K (2002) Long-term in vivo imaging of experience-dependent synaptic plasticity in adult cortex. Nature 420:788-794.
Tsai PS, Kleinfeld D (2009) In Vivo Two-Photon Laser Scanning Microscopy with Concurrent Plasma-Mediated Ablation Principles and Hardware Realization. In: In Vivo Optical Imaging of Brain Function, 2nd edition Edition (RD F, ed). Boca Raton (FL): CRC Press/Taylor & Francis.
Tsien RY (1998) The green fluorescent protein. Annual Review of Biochemistry 67:509-544.

Uchitel OD, Protti DA, Sanchez V, Cherksey BD, Sugimori M, Llinas R (1992) P-type voltage-dependent calcium channel mediates presynaptic calcium influx and transmitter release in mammalian synapses. Proceedings of the National Academy of Sciences of the United States of America 89:3330-3333.

Volgraf M, Gorostiza P, Numano R, Kramer RH, Isacoff EY, Trauner D (2006) Allosteric control of an ionotropic glutamate receptor with an optical switch. Nature Chemical Biology 2:47-52.

Vroom JM, De Grauw KJ, Gerritsen HC, Bradshaw DJ, Marsh PD, Watson GK, Birmingham JJ, Allison C (1999) Depth penetration and detection of pH gradients in biofilms by two-photon excitation microscopy. Applied and Environmental Microbiology 65:3502-3511.

Wachowiak M, Cohen LB (2001) Representation of odorants by receptor neuron input to the mouse olfactory bulb. Neuron 32:723-735.

Wang K, Horton NG, Xu C (2013) Going Deep: Brain Imaging with Multi-Photon Microscopy. Optics and Photonics News 24:32-39.

Wheeler GN, Brandli AW (2009) Simple Vertebrate Models for Chemical Genetics and Drug Discovery Screens: Lessons From Zebrafish and Xenopus. Developmental Dynamics 238:1287-1308.

White JG, Southgate E, Thomson JN, Brenner S (1986) The structure of the nervous system of the nematode Caenorhabditis elegans. Philosophical Transactions of the Royal Society of London Series B-Biological Sciences 314:1-340.

Williams FE, White D, Messer WS (2002) A simple spatial alternation task for assessing memory function in zebrafish. Behavioural Processes 58:125-132.

Wilt BA, Burns LD, Ho ETW, Ghosh KK, Mukamel EA, Schnitzer MJ (2009) Advances in Light Microscopy for Neuroscience. In: Annual Review of Neuroscience, pp 435-506. Palo Alto: Annual Reviews.

Wollebo HSW, Baheru.White, Martyn K. (2013) Lentiviral Transduction of Neuronal Cells. In: Neuronal Cell Culture, 1 Edition (Amini SW, Martyn K., ed), pp 141-146: Humana Press.

Xu C, Zipfel W, Shear JB, Williams RM, Webb WW (1996) Multiphoton fluorescence excitation: New spectral windows for biological nonlinear microscopy. Proceedings of the National Academy of Sciences of the United States of America 93:10763-10768.

Yaroslavsky AN, Schulze PC, Yaroslavsky IV, Schober R, Ulrich F, Schwarzmaier HJ (2002) Optical properties of selected native and coagulated human brain tissues in vitro in the visible and near infrared spectral range. Physics in Medicine and Biology 47:2059-2073.

Yuan F, Salehi HA, Boucher Y, Vasthare US, Tuma RF, Jain RK (1994) Vascular permeability and microcirculation of gliomas and mammary carcinomas transplanted in rat and mouse cranial windows. Cancer Research 54:4564-4568.

Zemelman BV, Nesnas N, Lee GA, Miesenbock G (2003) Photochemical gating of heterologous ion channels: Remote control over genetically designated populations of neurons. Proceedings of the National Academy of Sciences of the United States of America 100:1352-1357.

Zhang F, Wang LP, Boyden ES, Deisseroth K (2006) Channelrhodopsin-2 and optical control of excitable cells. Nature Methods 3:785-792.

Zhang F, Gradinaru V, Adamantidis AR, Durand R, Airan RD, de Lecea L, Deisseroth K (2010) Optogenetic interrogation of neural circuits: technology for probing mammalian brain structures. Nature Protocols 5:439-456.

Zhang F, Prigge M, Beyriere F, Tsunoda SP, Mattis J, Yizhar O, Hegemann P, Deisseroth K (2008) Red-shifted optogenetic excitation: a tool for fast neural control derived from Volvox carteri. Nature Neuroscience 11:631-633.

Zhang F, Wang LP, Brauner M, Liewald JF, Kay K, Watzke N, Wood PG, Bamberg E, Nagel G, Gottschalk A, Deisseroth K (2007) Multimodal fast optical interrogation of neural circuitry. Nature 446:633-U634.

Zipfel WR, Williams RM, Webb WW (2003) Nonlinear magic: multiphoton microscopy in the biosciences. Nature Biotechnology 21:1368-1376.

Ziv Y, Burns LD, Cocker ED, Hamel EO, Ghosh KK, Kitch LJ, El Gamal A, Schnitzer MJ (2013) Long-term dynamics of CA1 hippocampal place codes. Nature Neuroscience 16:264-266.